

# Divergence Frontiers for Generative Models: Sample Complexity, Quantization Level, and Frontier Integral

Lang Liu<sup>1</sup>

Krishna Pillutla<sup>2</sup>

Sean Welleck<sup>2,3</sup>

Sewoong Oh<sup>2</sup>

Yejin Choi<sup>2,3</sup>

Zaid Harchaoui<sup>1</sup>

<sup>1</sup> Department of Statistics, University of Washington

<sup>2</sup> Paul G. Allen School of Computer Science & Engineering, University of Washington

<sup>3</sup> Allen Institute for Artificial Intelligence

## Abstract

The spectacular success of deep generative models calls for quantitative tools to measure their statistical performance. Divergence frontiers have recently been proposed as an evaluation framework for generative models, due to their ability to measure the quality-diversity trade-off inherent to deep generative modeling. However, the statistical behavior of divergence frontiers estimated from data remains unknown to this day. In this paper, we establish non-asymptotic bounds on the sample complexity of the plug-in estimator of divergence frontiers. Along the way, we introduce a novel integral summary of divergence frontiers. We derive the corresponding non-asymptotic bounds and discuss the choice of the quantization level by balancing the two types of approximation errors arisen from its computation. We also augment the divergence frontier framework by investigating the statistical performance of smoothed distribution estimators such as the Good-Turing estimator. We illustrate the theoretical results with numerical examples from natural language processing and computer vision.

## 1 Introduction

Deep generative models have recently taken a giant leap forward in their ability to model complex, high-dimensional distributions. Recent advances are able to produce incredibly detailed and realistic images [27, 42, 25], strikingly consistent and coherent text [41, 58, 5], and music of near-human quality [12]. The advances in these models, particularly in the image domain, have been spurred by the development of quantitative evaluation tools which enable a large-scale comparison of models, as well as diagnosing of where and why a generative model fails [47, 31, 22, 46, 24].

The notion of a *divergence frontier* was recently proposed [14] to quantify the trade-off between quality and diversity arising in generative modeling with modern deep neural networks [46, 30, 51, 36, 14]. In particular, a good generative model must produce high-quality samples that are likely under the target distribution but must also cover the target distribution with diverse samples. While the framework is mathematically elegant and has found empirical success, the statistical properties of divergence frontiers are not well understood. Their estimation from data for large generative models involves two approximations: (a) joint quantization of the model and target distributions into discrete distributions with level  $k$ , and (b) estimation of the frontier between the quantized distributions from samples.

Djolonga et al. [14] argue that the quantization always introduces a positive bias, making the distributions appear closer than they really are; while a small sample size can result in a pessimistic estimate of the divergence frontier. The latter effect is due to the *missing mass* of the sample—the two distributions might appear farther than they really are because the samples do not cover some parts of the distributions. The first consideration favors a large  $k$ , while the second favors a small  $k$ .

In this paper, we are interested in answering the following questions: (i) Given two distributions, how many samples are needed to achieve a desired estimation accuracy, or in other words, what the sample complexity

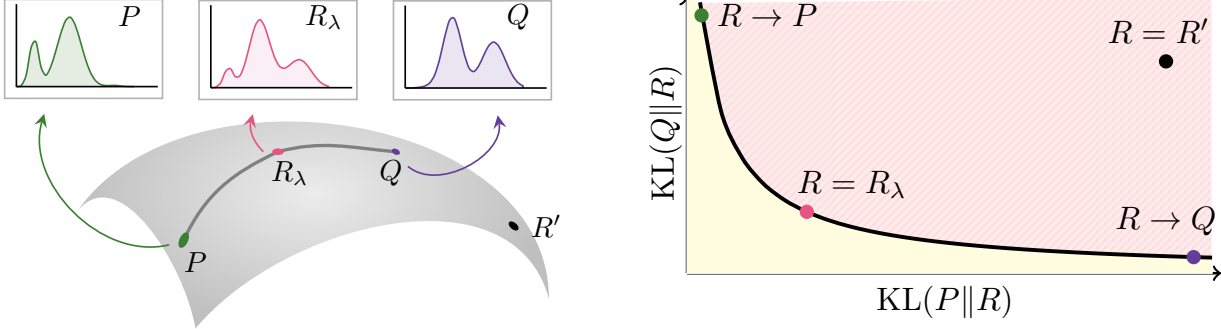


Figure 1: **Left:** Comparing two distributions  $P$  and  $Q$ . Here,  $R_\lambda = \lambda P + (1 - \lambda)Q$  is the interpolation between  $P$  and  $Q$  for  $\lambda \in (0, 1)$  and  $R'$  denotes some arbitrary distribution. **Right:** The corresponding divergence frontier (black curve) between  $P$  and  $Q$ . The interpolations  $R_\lambda$  for  $\lambda \in (0, 1)$  make up the frontier, while all other distributions such as  $R'$  must lie above the frontier.

of the estimation procedure is; (ii) Given a sample size budget, we ask how to choose the quantization level to balance the errors induced by the two approximations; (iii) We are interested in finding estimators better than the naïve plug-in estimator. The main contributions of the paper are:

- (a) We establish non-asymptotic bounds for the estimation of divergence frontiers, providing upper bounds on its sample complexity.
- (b) We propose a novel integral summary of divergence frontiers, derive corresponding non-asymptotic bounds and discuss the choice of the quantization level by balancing the errors induced by the two approximations.
- (c) We show both theoretically and empirically that smoothed distribution estimators, such as the add-constant estimator and the Good-Turing estimator, improve the estimation accuracy.
- (d) We demonstrate, through simulations on synthetic data as well as generative adversarial networks for images and transformer-based language models for text, that the bounds exhibit the correct dependence of the estimation error on the sample size  $n$  and the support size  $k$ .

As an added benefit, our analysis is transparent, and can be immediately generalized to a large class of  $f$ -divergences under some regularity assumptions. To bound the estimation error, we apply techniques from the missing mass literature to control the mass that never appears in the sample, and utilize the regularity properties of the  $f$ -divergence to bound the rest of them.

**Related work.** The most widely used metrics for generative models include Inception Score [47], Fréchet Inception Distance [22], and Kernel Inception Distance [3]. They summarize the performance by a single value and thus cannot distinguish different failure cases, i.e., low quality and low diversity. Motivated by this limitation, Sajjadi et al. [46] propose a metric to evaluate the quality of generative models using two separate components: precision and recall. This formulation is extended in [51] to arbitrary probability measures using a density ratio estimator, while alternative definitions based on non-parametric representations of the manifolds of the data were proposed in [30]. These notions are generalized by the divergence frontier framework of Djolonga et al. [14].

Another line of related work is the estimation of functionals of discrete distributions; see [54] for an overview. In particular, estimation of KL divergences has been studied by [7, 59, 6, 19] in the both fixed and large alphabet regimes. These results focus on the expected  $\mathbf{L}_1$  and  $\mathbf{L}_2$  risks and require additional assumptions on the two distributions such as boundedness of density ratio which is not needed in our results. On the practical side, there is a new line of successful work that uses deep neural networks to find data-dependent quantizations for the purpose of estimating information theoretic quantities from samples [45, 18].

**Notation.** Let  $\mathcal{P}(\mathcal{X})$  be the space of probability distributions on some measurable space  $\mathcal{X}$ . For any  $P, Q \in \mathcal{P}(\mathcal{X})$ , let  $\text{KL}(P\|Q)$  be the Kullback-Leibler (KL) divergence between  $P$  and  $Q$ . For  $\lambda \in (0, 1)$ , we define the *interpolated KL divergence* as  $\text{KL}_\lambda(P\|Q) := \text{KL}(P\|\lambda P + (1 - \lambda)Q)$ . For a partition  $\mathcal{S} := \{S_1, \dots, S_k\}$  of  $\mathcal{X}$ , we define  $P_{\mathcal{S}}$  the quantized version of  $P$  so that  $P_{\mathcal{S}} \in \mathcal{P}(\mathcal{S})$  with  $P_{\mathcal{S}}(S_i) = P(S_i)$  for any  $i \in [k] := \{1, \dots, k\}$ .

## 2 Divergence frontiers

Divergence frontiers compare two distributions  $P$  and  $Q$  using a frontier of statistical divergences. Each point on the frontier compares the individual distributions against a mixture  $R_\lambda$  of the two. By sweeping through mixtures, the curve interpolates between measurements of precision and recall. Figure 1 illustrates divergence frontiers, which we formally introduce below.

**Evaluating generative models via divergence frontiers.** Consider a generative model  $Q \in \mathcal{P}(\mathcal{X})$  which attempts to model the target distribution  $P \in \mathcal{P}(\mathcal{X})$ . It has been argued in [30, 46] that one must consider two types of errors to evaluate  $Q$  with respect to  $P$ : (a) a loss in precision, which is the mass of  $P$  that  $Q$  does not adequately capture, and, (b) a loss in recall, which is the mass of  $Q$  that has low or zero probability mass under  $P$ .

Suppose  $P, Q$  are uniform distributions on their supports, and  $R$  is uniform on the union of their supports. Then, the loss in precision is the mass of  $\text{Supp}(Q) \setminus \text{Supp}(P)$ , or equivalently, the mass of  $\text{Supp}(R) \setminus \text{Supp}(P)$ . We measure this using the surrogate  $\text{KL}(Q\|R)$ , which is large if there exists  $a$  such that  $Q(a)$  is large but  $R(a)$  is small. Likewise, the loss in recall is measured by  $\text{KL}(P\|R)$ . When  $P$  and  $Q$  are not constrained to be uniform, it is not clear what the measure  $R$  should be. Djolonga et al. [14] propose to vary  $R$  over all possible probability measures and consider the Pareto frontier of the multi-objective optimization  $\min_R (\text{KL}(P\|R), \text{KL}(Q\|R))$ . This leads to a curve called the *divergence frontier*, and is reminiscent of the precision-recall curve in binary classification.

Formally, it can be shown that the divergence frontier  $\mathcal{F}(P, Q)$  of probability measures  $P, Q$  is carved out by mixtures  $R_\lambda = \lambda P + (1 - \lambda)Q$  for  $\lambda \in (0, 1)$  (cf. Figure 1). It admits the closed-form

$$\mathcal{F}(P, Q) = \left\{ (\text{KL}_\lambda(P\|Q), \text{KL}_{1-\lambda}(Q\|P)) : \lambda \in (0, 1) \right\},$$

where  $\text{KL}_\lambda(P\|Q) = \text{KL}(P\|\lambda P + (1 - \lambda)Q)$  is the interpolated KL divergence.

**Practical computation of divergence frontiers.** In practical applications,  $P$  is a complex, high-dimensional distribution which could either be discrete, as in natural language processing, or continuous, as in computer vision. Likewise,  $Q$  is often a deep generative model such as GPT-3 for text and GANs for images. It is infeasible to compute the divergence frontier  $\mathcal{F}(P, Q)$  directly because we only have samples from  $P$  and the integrals or sums over  $Q$  are intractable.

Therefore, the recipe used by practitioners [46, 14] has been to (a) jointly quantize  $P$  and  $Q$  over a partition  $\mathcal{S} = \{S_1, \dots, S_k\}$  of  $\mathcal{X}$  to obtain discrete distributions  $P_{\mathcal{S}} = (P(S_1), \dots, P(S_k))$  and  $Q_{\mathcal{S}} = (Q(S_1), \dots, Q(S_k))$ , (b) estimate the quantized distributions from samples to get  $\hat{P}_{\mathcal{S}}$ ,  $\hat{Q}_{\mathcal{S}}$ , and (c) compute  $\mathcal{F}(\hat{P}_{\mathcal{S}}, \hat{Q}_{\mathcal{S}})$ . In practice, the best quantization schemes are data-dependent transformations such as  $k$ -means clustering or lattice-type quantization of dense representations of images or text [45].

**Scalar summary of divergence frontiers.** Since it can be cumbersome to compare divergence frontiers  $\mathcal{F}(P, Q_j)$  for a number of models  $Q_1, Q_2, \dots$ , it is beneficial to summarize the frontier with a scalar. It can also be used to quantify the convergence of the divergence frontier over all  $\lambda$ .

We define a novel integral summary, called the *frontier integral*  $\text{FI}(P, Q)$  of two distributions  $P, Q$  as

$$\text{FI}(P, Q) := 2 \int_0^1 (\lambda \text{KL}_\lambda(P\|Q) + (1 - \lambda) \text{KL}_{1-\lambda}(Q\|P)) \, d\lambda. \quad (1)$$

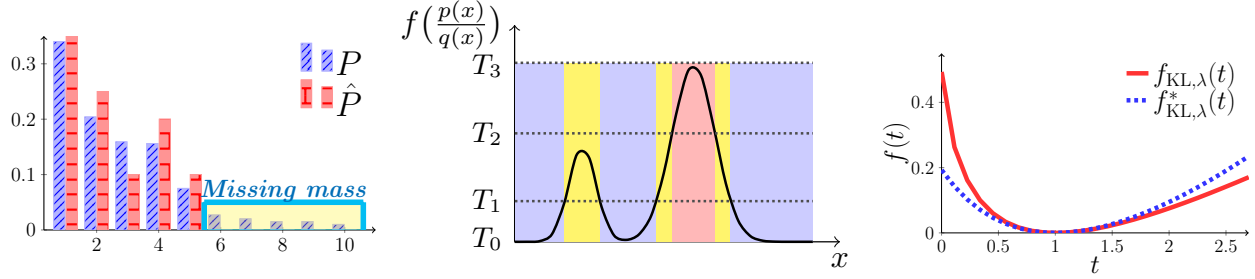


Figure 2: **Left:** The missing mass in a sample. **Middle:** Oracle quantization into 3 bins: blue, yellow and red. Bin  $i$  is given by the set  $\{x : f(p(x)/q(x)) \in [T_{i-1}, T_i]\}$ . **Right:** The generator and conjugate generator of  $\text{KL}_\lambda$  at  $\lambda = 1/2$ .

We can interpret the frontier integral as the average value of the scalarized objective which defines each point on the divergence frontier.

While the length of the divergence frontier could be unbounded (e.g., when  $\text{KL}(P\|Q)$  is unbounded), the frontier integral is always bounded in  $[0, 1]$ . Moreover, it is a symmetric divergence with  $\text{FI}(P, Q) = 0$  if and only if  $P = Q$ . In practice, the frontier integral can be estimated using the same recipe as the divergence frontier.

**Error decomposition.** In Section 3, we decompose the error in estimating the frontier integral into two components: the statistical error of estimating the quantized distribution and the quantization error. Our goal is to derive the rate of convergence for the overall estimation error. To control the statistical error, we use a different treatment for the masses that appear in the sample and the ones that never appear (i.e., the missing mass). We obtain a high probability bound as well as a bound for its expectation, leading to upper bounds for its sample complexity and rate of convergence. These results carry over to the divergence frontiers as well. As for the quantization error, we construct a distribution-dependent quantization scheme whose error is at most  $O(k^{-1})$ , where  $k$  is the quantization level. A combination of these two bounds sheds light on the optimal choice of the quantization level. In Section 5, we verify empirically the tightness of the rates on synthetic and real data.

### 3 Main results

Let  $P, Q \in \mathcal{P}(\mathcal{X})$ . Let  $\{X_i\}_{i=1}^n$  and  $\{Y_i\}_{i=1}^n$  be independent i.i.d. samples from  $P$  and  $Q$ , respectively. Denote by  $\hat{P}_n$  and  $\hat{Q}_n$  the respective empirical measures of  $P$  and  $Q$ . Note that the two samples are assumed to have the same size for simplicity. In this section, we summarize our main theoretical results. We denote by  $C$  an absolute constant which can vary from line to line. The precise statements and proofs can be found in the Appendix.

**Sample complexity for the frontier integral.** We are interested in deriving a non-asymptotic bound for the absolute error of the plug-in estimator, i.e.,  $|\text{FI}(\hat{P}_n, \hat{Q}_n) - \text{FI}(P, Q)|$ . When both  $P$  and  $Q$  are supported on a finite alphabet with  $k$  items, a natural strategy is to exploit the smoothness properties of FI, giving a naïve upper bound  $O(L\sqrt{k/n})$  on the absolute error, where  $L = \log 1/p_*$  with  $p_* = \min_{a \in \text{Supp}(P)} P(a)$  reflecting the smoothness of FI. The dependency on  $p_*$  requires  $P$  to have a finite support and a short tail. However, in many real-world applications, the distributions can either be supported on a (countably) infinitely large set or have long tails [9, 56]. By considering the *missing mass* in the sample, we are able to obtain a high probability bound that is independent of  $p_*$ .

**Theorem 1.** Assume that  $P$  and  $Q$  are discrete and let  $k = \max\{|\text{Supp}(P)|, |\text{Supp}(Q)|\} \in \mathbb{N} \cup \{\infty\}$ . For any  $\delta \in (0, 1)$ , it holds that, with probability at least  $1 - \delta$ ,

$$|\text{FI}(\hat{P}_n, \hat{Q}_n) - \text{FI}(P, Q)| \leq C \left[ \left( \sqrt{\frac{\log 1/\delta}{n}} + \alpha_n(P) + \alpha_n(Q) \right) \log n + \beta_n(P) + \beta_n(Q) \right], \quad (2)$$

where  $\alpha_n(P) = \sum_{a \in \mathcal{X}} \sqrt{n^{-1}P(a)}$  and  $\beta_n(P) = \mathbb{E} \left[ \sum_{a: \hat{P}_n(a)=0} P(a) \max \{1, \log(1/P(a))\} \right]$ . Furthermore, if the support size  $k < \infty$ , then  $\alpha_n(P) \leq \sqrt{k/n}$  and  $\beta_n(P) \leq k \log n/n$ . In particular, with probability at least  $1 - \delta$ ,

$$|\text{FI}(\hat{P}_n, \hat{Q}_n) - \text{FI}(P, Q)| \leq C \left[ \sqrt{\frac{\log 1/\delta}{n}} + \sqrt{\frac{k}{n}} + \frac{k}{n} \right] \log n. \quad (3)$$

Before we discuss the bounds in Theorem 1, let us introduce the missing mass problem. This problem was first studied by Good and Turing [16], where the eponymous Good-Turing estimator was proposed to estimate the probability that a new observation drawn from a fixed distribution has never appeared before, in other words, is missing in the current sample; see Figure 2 (left) for an illustration. The Good-Turing estimator has been widely used in language modeling [26, 10, 9] and studied in theory [34, 40, 39]. An inspiring result coming from this line of work is that the missing mass in a sample of size  $n$  concentrates around its expectation [33], which itself decays as  $O(k/n)$  when the distribution is supported on  $k$  items [2].

There are several merits to Theorem 1. First, (2) holds for any distributions with a countable support. Second, it does not depend on  $p_*$  and is adapted to the tail behavior of  $P$  and  $Q$ . For instance, if  $P$  is defined as  $P(a) \propto a^{-2}$  for  $a \in [k]$ , then  $\alpha_n(P) \propto (\log k)/\sqrt{n}$ , which is much better than  $\sqrt{k/n}$  in (3) in terms of the dependency on  $k$ . This phenomenon is also demonstrated empirically in Section 5. Third, it captures a parametric rate of convergence, i.e.,  $O(n^{-1/2})$ , up to a logarithmic factor. In fact, this rate is not improvable in a related problem of estimating  $\text{KL}(P\|Q)$ , even with the assumption that  $P/Q$  is bounded [6]. The bound in (3) is a distribution-free bound, assuming  $k$  is finite. Note that it also gives an upper bound on the sample complexity by setting the right hand side of (4) to be  $\epsilon$  and solve for  $n$ , this is roughly  $O((\sqrt{\log 1/\delta} + \sqrt{k})^2/\epsilon^2)$ .

*Proof sketch of Theorem 1.* The proof of Theorem 1 relies on two new results: (a) a concentration bound around  $\mathbb{E}[\text{FI}(\hat{P}_n, \hat{Q}_n)]$ , which can be obtained by McDiarmid's inequality, and (b) an upper bound for the statistical error, i.e.,  $\mathbb{E}|\text{FI}(\hat{P}_n, \hat{Q}_n) - \text{FI}(P, Q)|$ , which we show that it is upper bounded by

$$O([\alpha_n(P) + \alpha_n(Q)] \log n + \beta_n(P) + \beta_n(Q)) \leq O((\sqrt{k/n} + k/n) \log n). \quad (4)$$

We show in Proposition 6 (Appendix B) that the frontier integral is an  $f$ -divergence with generator  $f_{\text{FI}}$ :

$$\text{FI}(P, Q) = \sum_{a \in \text{Supp}(P)} Q(a) f_{\text{FI}}(P(a), Q(a)) =: \sum_{a \in \text{Supp}(P)} \psi(P(a), Q(a)). \quad (5)$$

Define  $\Delta_n(a) := |\psi(P(a), Q(a)) - \psi(\hat{P}_n(a), \hat{Q}_n(a))|$ . The triangle inequality yields  $|\text{FI}(P, Q) - \text{FI}(\hat{P}_n, \hat{Q}_n)| \leq \sum_{a \in \text{Supp}(P)} \Delta_n(a)$  and

$$\Delta_n(a) \leq \underbrace{|\psi(P(a), Q(a)) - \psi(\hat{P}_n(a), Q(a))|}_{=: \mathcal{T}_1(a)} + \underbrace{|\psi(\hat{P}_n(a), Q(a)) - \psi(\hat{P}_n(a), \hat{Q}_n(a))|}_{=: \mathcal{T}_2(a)}.$$

We can show that  $\psi$  is approximately Lipschitz (Lemma 2) so that

$$\mathcal{T}_1(a) \leq \begin{cases} C P(a) \max\{1, \log 1/P(a)\} & \text{if } \hat{P}_n(a) = 0, \\ C |P(a) - \hat{P}_n(a)| \log n & \text{else.} \end{cases}$$

The part for  $\hat{P}_n(a) = 0$  leads to the term  $\beta_n(P)$ , which falls into the missing mass framework and can be further upper bounded by  $O(k/n \log n)$ . Note that this rate matches the rate for the missing mass up to a logarithmic factor. The part for  $\hat{P}_n(a) > 0$  can be controlled by considering the second moment of  $P(a) - \hat{P}_n(a)$ , giving the term  $O(\alpha_n(P) \log n) \leq O(\sqrt{k/n} \log n)$ . An analogous bound holds for  $\mathcal{T}_2$  by symmetry of FI and thus the bound in (4) holds.

The concentration bound can be obtained similarly using the approximate Lipschitz lemma and McDiarmid's inequality, and it gives the term  $\sqrt{n^{-1} \log 1/\delta}$ .  $\square$

**Lemma 2** (Approximate Lipschitz). *Consider  $\psi$  from (5). For all  $p, p' \in [0, 1]$  with  $\max\{p, p'\} > 0$ , we have*

$$|\psi(p', q) - \psi(p, q)| \leq C \max \left\{ 1, \log \frac{1}{\max\{p, p'\}} \right\} |p - p'|$$

**Statistical consistency of the divergence frontiers.** While Theorem 1 establishes the consistency of the frontier integral, it is also of great interest to know whether the divergence frontier itself can be consistently estimated. In fact, a similar bound holds for  $\text{KL}_\lambda(\hat{P}_n \parallel \hat{Q}_n)$ , with the rate  $O(\lambda^{-1} \sqrt{k/n} \log n)$  for each  $\lambda \in (0, 1)$ . Furthermore, if we truncate the frontier within the interval  $[\lambda_n, 1 - \lambda_n]$  for some  $\lambda_n \rightarrow 0$ , then the truncated empirical frontier converges uniformly to its population counterpart at rate  $O(\lambda_n^{-1} \sqrt{k/n} \log n)$ . The truncation is necessary without imposing additional assumptions, since  $\text{KL}_\lambda$  is close to  $\text{KL}$  for small  $\lambda$  and it is known that the minimax quadratic risk of estimating the KL divergence over all distributions with  $k$  bins is always infinity [6].

**Upper bound for the quantization error.** Recall from Section 2 that computing the divergence frontiers in practice usually involves a quantization step. Since every quantization will inherently introduce a bias in the estimation procedure, it is desirable to control the error, which we call the quantization error, induced by this step. We show that there exists a quantization scheme with error proportional to the inverse of its size. We implement this scheme and empirically verify this rate in section 5; certain regimes appear to show even faster convergence.

Let  $\mathcal{X}$  be an *arbitrary* measurable space and  $\mathcal{S}$  be a partition of  $\mathcal{X}$ . The quantization error of  $\mathcal{S}$  is the difference  $|\text{FI}(P_{\mathcal{S}}, Q_{\mathcal{S}}) - \text{FI}(P, Q)|$ . It can be shown that there exists a distribution-dependent partition  $\mathcal{S}_k$  with level  $|\mathcal{S}_k| = k$  whose quantization error is no larger than the inverse of its level, i.e.,

$$|\text{FI}(P, Q) - \text{FI}(P_{\mathcal{S}_k}, Q_{\mathcal{S}_k})| \leq Ck^{-1}. \quad (6)$$

Combining this bound with the bounds in (4) leads to the following bound for the overall estimation error.

**Theorem 3.** *Assume that  $\mathcal{S}_k$  is a partition of  $\mathcal{X}$  such that  $|\mathcal{S}_k| = k \geq 2$  and its quantization error satisfies the bound in (6). Then*

$$\begin{aligned} \mathbb{E} \left| \text{FI}(\hat{P}_{\mathcal{S}_k, n}, \hat{Q}_{\mathcal{S}_k, n}) - \text{FI}(P, Q) \right| &\leq C \left[ (\alpha_n(P) + \alpha_n(Q)) \log n + \beta_n(P) + \beta_n(Q) + k^{-1} \right] \\ &\leq C \left[ \left( \sqrt{\frac{k}{n}} + \frac{k}{n} \right) \log n + \frac{1}{k} \right]. \end{aligned} \quad (7)$$

*Proof sketch of Theorem 3.* By the triangle inequality, it holds that

$$\mathbb{E} |\text{FI}(\hat{P}_{\mathcal{S}_k, n}, \hat{Q}_{\mathcal{S}_k, n}) - \text{FI}(P, Q)| \leq \mathbb{E} |\text{FI}(\hat{P}_{\mathcal{S}_k, n}, \hat{Q}_{\mathcal{S}_k, n}) - \text{FI}(P_{\mathcal{S}_k}, Q_{\mathcal{S}_k})| + \mathbb{E} |\text{FI}(P_{\mathcal{S}_k}, Q_{\mathcal{S}_k}) - \text{FI}(P, Q)|.$$

The first term can be upper bounded by the statistical error bound in (4). To control the second term, we construct a partition  $\mathcal{S}_k$  of  $\mathcal{X}$  which satisfies (6).

To begin with, we note that the generator  $f_{\text{FI}}$  to the Frontier integral is bounded by  $f_{\text{FI}}(0)$  on the subset

$$\mathcal{X}_1 = \left\{ x \in \mathcal{X} : \frac{dP}{dQ}(x) \leq 1 \right\}.$$

This subset can be partitioned into  $\lfloor k/2 \rfloor$  bins based on the value of  $f_{\text{FI}}(dP/dQ)$ . Concretely, we define

$$S_m = \left\{ x \in \mathcal{X}_1 : \frac{f_{\text{FI}}(0)(m-1)}{\lfloor k/2 \rfloor} \leq f_{\text{FI}} \left( \frac{dP}{dQ}(x) \right) < \frac{f_{\text{FI}}(0)m}{\lfloor k/2 \rfloor} \right\}, \quad \text{for } m \in \{1, \dots, \lfloor k/2 \rfloor\}.$$

This idea is visualized in Figure 2 (middle). It can be shown that the quantization error in each bin  $S_m$  is at most  $f_{\text{FI}}(0)Q[\mathcal{S}_m]/k$ . Adding them up contributes to a term  $f_{\text{FI}}(0)/k$  in the bound (6). For the subset  $\mathcal{X}_2 = \{x \in \mathcal{X} : \frac{dP}{dQ}(x) > 1\}$ , it can be partitioned analogously by considering the conjugate generator  $f_{\text{FI}}^*$ .  $\square$

Based on the bound in (7), a good choice of  $k$  is  $\Theta(n^{1/3})$  which balances between the two types of errors. We illustrate in Section 5 that our experimental results approximately conform to the scaling observed from Theorem 3 by investigating the two errors separately. This balancing is enabled by the existence of a good quantizer with a distribution-free bound in (6). In practice, this suggests a data-dependent quantizer using nonparametric density estimators. However, directions such as kernel density estimators [43, 21, 53] and nearest-neighbor methods [1] have not met with empirical success, as they suffer from the curse of dimensionality common in nonparametric estimators. In particular, [55, 49, 50] propose quantized divergence estimators but only prove asymptotic consistency, and little progress has been made since then. On the other hand, modern data-dependent quantization techniques based on deep neural networks can successfully estimate properties of the density from high dimensional data [45, 18]. Theoretical results for those techniques could complement our analysis. We leverage these powerful methods to scale our approach on real data in Section 5.2.

## 4 Towards better estimators and interpolated $f$ -divergences

**Smoothed distribution estimators.** When the support size  $k$  is large, the statistical performance of the direct estimator considered in the previous section can be improved. To overcome this challenge, practitioners often use more sophisticated distribution estimators such as the Good-Turing estimator [16, 39] and add-constant estimators [28, 4]. We focus on the add-constant estimator defined below and state here its estimation error when it is applied to estimate the frontier integral from data. We investigate and compare the performance of other distribution estimators in Section 5.

For notational simplicity, we assume that  $P$  and  $Q$  are supported on a common finite alphabet with size  $k < \infty$ . Note that this is true for the quantized distributions  $P_S$  and  $Q_S$ . For any constant  $b > 0$ , the add-constant estimator of  $P$  is defined as  $\hat{P}_{n,b}(a) = (N_a + b)/(n + kb)$  for each  $a \in \text{Supp}(P)$ , where  $N_a = |\{i : X_i = a\}|$  is the number of times  $a$  appears in the sample. The add-constant estimator of  $Q$  is defined analogously.

Thanks to the smoothing, there is no mass missing in the add-constant estimator. As a result, we can directly utilize the smoothness properties of the frontier integral to get the following bound.

**Proposition 4.** *Under the same assumptions as in Theorem 3, we have*

$$\begin{aligned} & \mathbb{E} \left| \text{FI}(\hat{P}_{S_k, n, b}, \hat{Q}_{S_k, n, b}) - \text{FI}(P, Q) \right| \\ & \leq C \left[ \left( \frac{n(\alpha_n(P) + \alpha_n(Q))}{n + bk} + \gamma_{n,k}(P) + \gamma_{n,k}(Q) \right) \log(n/b + k) + \frac{1}{k} \right] \\ & \leq C \left[ \frac{\sqrt{nk} + bk}{n + bk} \log(n/b + k) + \frac{1}{k} \right], \end{aligned} \tag{8}$$

where  $\gamma_{n,k}(P) = (n + bk)^{-1}bk \sum_{a \in \mathcal{X}} |P(a) - 1/k|$ .

Let us compare the bounds in Proposition 4 with the ones in Theorem 3. For the distribution-dependent bound, the term  $\alpha_n(P) \log n$  in (7) is improved by a factor  $n/(n + bk)$  in (8). The missing mass term  $\beta_n(P)$  is replaced by the total variation distance between  $P$  and the uniform distribution on  $[k]$  with a

factor  $bk/(n + bk)$ . The improvements in both two terms are most significant when  $k/n$  is large. As for the distribution-free bound, when  $k/n$  is small, the bound in (8) scales the same as the one in (7); when  $k/n$  is large (i.e., bounded away from 0 or diverging), it scales as  $O(\log n + \log(k/n) + k^{-1})$  while the one in (7) scales as  $O(k \log n/n + k^{-1})$ . Given the improvement, it would be an interesting venue for future work to consider adaptive estimators in the spirit of [15].

**Generalization to  $f$ -divergences.** Estimation of the  $\chi^2$  divergence is useful for variational inference [13] and GAN training [32, 52]. More generally, estimating  $f$ -divergences from samples is a fundamental problem in machine learning and statistics [37, 23, 8, 44]. We extend our previous results to estimating general  $f$ -divergences (which satisfy some regularity assumptions) using the same two-step procedure of quantization and estimation of multinomial distributions from samples.

We start by reviewing the definition of  $f$ -divergences; see Appendix A for more details. Let  $f : (0, \infty) \rightarrow \mathbb{R}$  be a nonnegative and convex function with  $f(1) = 0$ . Let  $P, Q \in \mathcal{P}(\mathcal{X})$  be dominated by some measure  $\mu \in \mathcal{P}(\mathcal{X})$  with densities  $p$  and  $q$ , respectively. The  $f$ -divergence generated by  $f$  is defined as

$$D_f(P\|Q) = \int_{\mathcal{X}} q(x) f\left(\frac{p(x)}{q(x)}\right) d\mu(x),$$

with the convention that  $f(0) = f(0^+)$  and  $0f(p/0) = pf^*(0)$ , where  $f^*(0) = f^*(0^+) \in [0, \infty]$  for  $f^*(t) = tf(1/t)$ . We call  $f^*$  the conjugate generator to  $f$ . Note that the conjugacy here is unrelated to the convex conjugacy but is based on the *perspective transform*. The function  $f^*$  also generates an  $f$ -divergence, which is referred to as the *conjugate divergence* to  $D_f$  since  $D_{f^*}(P\|Q) = D_f(Q\|P)$ .

The quantization error bound (6) holds for all  $f$ -divergences which are *bounded*, i.e.,  $f(0) + f^*(0) < \infty$ . The high probability bounds in Theorem 1 also hold for general  $f$ -divergences, under some regularity assumptions. The interpolated  $\chi^2$  divergence, defined analogously as the interpolated KL divergence, satisfies these conditions. In addition to the boundedness assumption, we assume  $|f'(t)| \propto \log t^{-1}$  and  $|f^*(t)| \propto \log t^{-1}$  for small  $t$ . This guarantees that  $f$  is approximately Lipschitz in the sense of Lemma 2 and cannot vary too fast. We also require a technical assumption that helps control the variation of  $f$  around zero, namely that  $t f''(t)$  and  $t(f^*)''(t)$  are bounded.

Both the interpolated KL divergence and the frontier integral are  $f$ -divergences satisfying the regularity conditions. An illustration of the generator to  $\text{KL}_{1/2}$  can be found in Figure 2 (right). Hence, Theorem 1, Theorem 3 and Proposition 4 are special cases of the corresponding results for  $f$ -divergences.

## 5 Experiments

We investigate the empirical behavior of the frontier integral on both synthetic and real data. Our main findings are: 1) the statistical error bound is tight—it approximately reveals the rate of convergence of the plug-in estimator. 2) The smoothed distribution estimators improve the estimation accuracy. We summarize our experimental settings and findings here. More details and additional results are deferred to Appendix G.

### 5.1 Synthetic data

**Settings.** We focus on the case when  $k = |\mathcal{X}| < \infty$ . Following the experimental settings in [39], we consider three types of distributions: 1) the Zipf( $r$ ) distribution with  $r \in \{0, 1, 2\}$  where  $P(i) \propto i^{-r}$ . Note that Zipf( $r$ ) is regularly varying with index  $-r$ ; see, e.g., [48, Appendix B]. 2) the Step distribution where  $P(i) = 1/2$  for the first half bins and  $P(i) = 3/2$  for the second half bins. 3) the Dirichlet distribution  $\text{Dir}(\alpha)$  with  $\alpha \in \{\mathbf{1}/2, \mathbf{1}\}$ . In total, there are 6 different distributions. Since the frontier integral is symmetric, there are 21 different pairs of  $(P, Q)$ . For each pair  $(P, Q)$ , we generate i.i.d. samples of size  $n$  from each of them, and then compute the absolute error  $|\text{FI}(\hat{P}_n, \hat{Q}_n) - \text{FI}(P, Q)|$ . We repeat the process 100 times and report its mean and standard error, which is referred to as the Monte Carlo estimate of the expected absolute error.

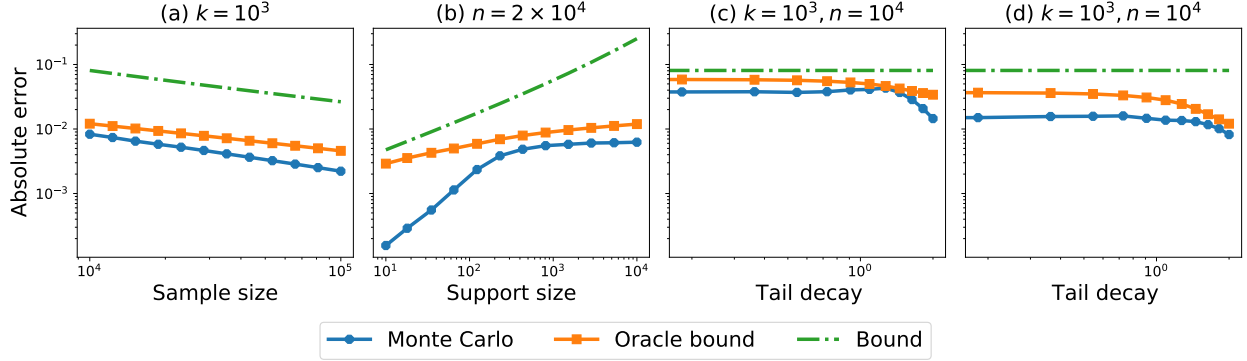


Figure 3: Statistical error bounds (4) and the Monte Carlo estimate (log-log scale). (a): Zipf(2) and Zipf(2) with  $k = 10^3$ ; (b): Zipf(2) and Zipf(2) with  $n = 2 \times 10^4$ ; (c): Dir(1) and Zipf( $r$ ) with  $k = 10^3$  and  $n = 10^4$ ; (d): Zipf(2) and Zipf( $r$ ) with  $k = 10^3$  and  $n = 10^4$ . The bounds are scaled by 100.

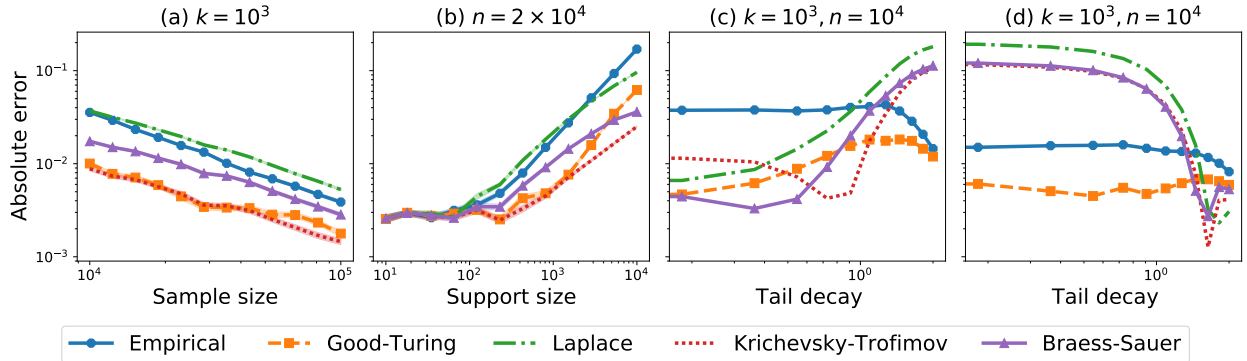


Figure 4: Absolute error for different distribution estimators (log-log scale). (a): Zipf(0) and Dir(1/2) with  $k = 10^3$ ; (b): Zipf(0) and Dir(1/2) with  $n = 2 \times 10^4$ ; (c): Dir(1) and Zipf( $r$ ) with  $k = 10^3$  and  $n = 10^4$ ; (d): Zipf(2) and Zipf( $r$ ) with  $k = 10^3$  and  $n = 10^4$ .

**Statistical error.** To study the tightness of the statistical error bounds (4), we compare both the distribution-free bound (“bound”) and the distribution-dependent bound (“oracle bound”) with the Monte Carlo estimate. We consider three different experiments. First, we fix the support size  $k = 10^3$  and increase the sample size  $n$  from  $10^3$  to  $10^4$ . Second, we fix  $n = 2 \times 10^4$  and increase  $k$  from 10 to  $10^4$ . Third, we fix  $k = 10^3$  and  $n = 10^4$ , and set  $Q$  to be the Zipf( $r$ ) with  $r$  ranging from 0 to 2. We report four plots in Figure 3; see Appendix G for more results. Note that the two bounds are divided by the same constant 100 for the sake of comparison.

As shown in Figure 3(a), the two bounds and the Monte Carlo estimate exhibit a near-identical rate in  $n$ . In some cases, the Monte Carlo estimate demonstrates a faster rate of convergence than the bounds. This suggests that the bounds capture the worst-case behavior of the plug-in estimator. In the second experiment, we observe in Figure 3(b) that the oracle bound exhibits a slower rate than the bound in  $k$ . The Monte Carlo estimate has a near identical rate as the bound for small  $k$  and a near-identical rate as the oracle bound for large  $k$ . Figures 3(c) and 3(d) show that, while the bound remains the same for different tails of  $Q$ , the oracle bound is adapted to the decaying index of  $Q$  and captures well the behavior of the Monte Carlo estimate.

**Distribution estimators.** We then compare 4 distribution estimators with the empirical measures (“Empirical”) as discussed in [39]—the (modified) *Good-Turing* estimator and three add-constant estimators, namely, the *Laplace* estimator, the *Krichevsky-Trofimov* estimator and the *Braess-Sauer* estimator. Their precise definitions can be found in Appendix G. We consider the same three experiments as for the statistical error. As shown in Figures 4(a) and 4(b), the rates in  $n$  and  $k$  are similar across all estimators, and the

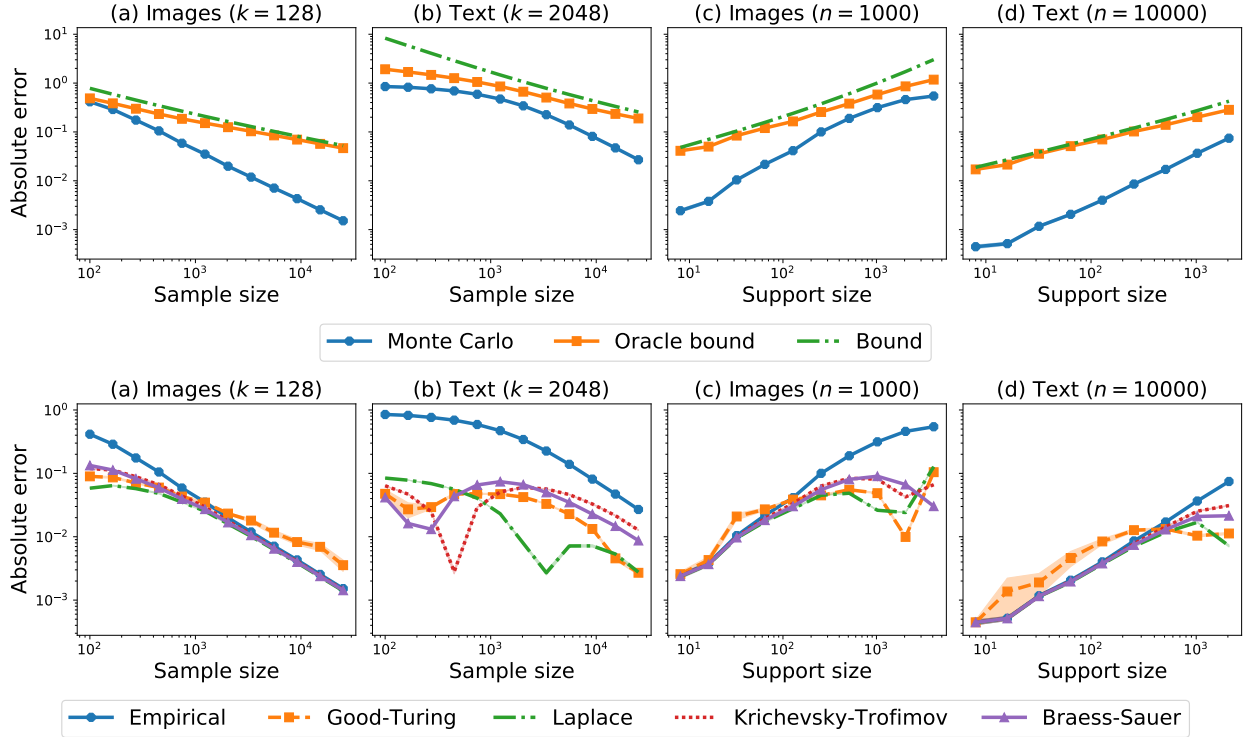


Figure 5: Absolute error for the statistical error bounds (**top**) and different distribution estimators (**bottom**) (log-log scale). **(a)**: Image data (CIFAR-10) with  $k = 128$ ; **(b)**: Text data (WikiText-103) with  $k = 2048$ ; **(c)**: Image data (CIFAR-10) with  $n = 1000$ ; **(d)**: Text data (WikiText-103) with  $n = 10000$ . The bounds are scaled by 15.

Krichevsky-Trofimov estimator and the Good-Turing estimator outperform others. Furthermore, we observe from additional results in Appendix G that when two distributions are the same, all estimators performs similarly with the Good-Turing estimator being the worst. Next, we observe in Figures 4(c) and 4(d) that the add-constant estimators perform worse than the empirical one for some tail-decaying regimes; while the Good-Turing estimator is relatively robust to the tail decay in  $Q$ .

**Quantization error.** We consider three quantization strategies: 1) the uniform quantization which partitions the distributions into equally spaced bins; 2) the greedy quantization which sorts the bins according to the ratios  $\{P(a)/Q(a)\}_{a \in \mathcal{X}}$  and then add one bin at a time so that the frontier integral is maximized; 3) the oracle quantization we used to prove (6); see Figure 2. Due to space limit, we defer the results to Appendix G. We observe that when both  $P$  and  $Q$  have slow-decaying tails, the absolute error of the oracle quantization decays faster than  $O(k^{-1})$ ; when one of them has fast-decaying tail, its absolute error decays slower than  $O(k^{-1})$  in the beginning and then faster than  $O(k^{-1})$ . In our experiments, the oracle quantization always outperforms the greedy one. When either  $P$  or  $Q$  is not ordered, the uniform quantization performs the worst. When both  $P$  and  $Q$  are ordered, its absolute error is quite small in the beginning and then becomes larger.

## 5.2 Real data

We analyze the bounds as well as the distribution estimators in the context evaluating generative models for images and text using divergence frontiers.

**Tasks and Datasets.** We consider two domains: images and text. For the image domain, we train a generative model for the CIFAR-10 dataset [29] based on StyleGAN2 [25]. We use the publicly available code<sup>1</sup> with their default hyperparameters and train on 2 GPUs. To evaluate the frontier integral, we use the test set of 10k images as the target distribution  $P$  and we sample 10k images from the generative model as the model distribution  $Q$ . For the text domain, we fine-tune a pretrained GPT-2 [41] model with 124M parameters (i.e., GPT-2 small) on the Wikitext-103 dataset [35]. We use the open-source HuggingFace Transformers library [57] for training, and generate 10k 500-token completions using top- $p$  sampling and 100-token prefixes.

**Settings.** We take the following steps to compute the frontier integral. First, we represent each image/text by its features [22, 46, 30]. Second, we learn a low-dimensional feature embedding which maintains the neighborhood structure of the data while encouraging the features to be uniformly distributed on the unit sphere [45]. Third, we quantize these embeddings on a uniform lattice with  $k$  bins. For each support size  $k$ , this gives us quantized distributions  $P_{\mathcal{S}_k}, Q_{\mathcal{S}_k}$ . Finally, we sample  $n$  i.i.d observations each from these distributions and consider the empirical distributions  $\hat{P}_{\mathcal{S}_k, n}, \hat{Q}_{\mathcal{S}_k, n}$  as well as the add-constant and Good-Turing estimators computed from these samples.

**Statistical error.** Following the corresponding part on synthetic data, we consider two experiments. First, we fix the support size  $k$  and vary the sample size  $n$  from 100 to 25000. Second, we fix the sample size  $n$  and vary the support size  $k$  from 8 to 2048 in powers of 2. The findings are similar—the bounds capture the worst-case behavior in  $n$  of real image and text data, and, in  $k$ , the Monte Carlo estimate can grows either at a similar rate or faster than the bounds depending on the value of  $n$ .

**Distribution Estimators.** As in the previous section, we compare the empirical estimator with four distribution estimators. From Figure 5 (bottom), we observe similar rates (i.e., similar slopes) for all estimators with respect to the sample size  $n$  when  $n > k$ . The absolute error of the Good-Turing estimator is the worst among all estimators considered for  $k = 128$  and  $n$  large. However, for  $k = 2048$ , the empirical estimator is the worst. The various add- $b$  estimators work the best in the regime of  $n < k$ , where each add- $b$  estimator attains the smallest error at a different  $n$ . In particular, the Laplace estimator is the best or close to the best in all each of the settings considered.

**Performance across training.** Next, we visualize the divergence frontiers and the corresponding frontier integral across training in Figure 7. On the left, we plot the divergence curve at initialization (or with the pretrained model in case of text), at the first checkpoint (“Partly”) and the fully trained model (“Final”). We observe that the divergence frontiers for the fully trained model are closer to the origin than the partially trained ones or the model at initialization. This denotes a smaller loss of precision and recall for the fully trained model. The frontier integral, as a summary statistic, shows the same trend (right).

## 6 Conclusion

In this paper, we study the statistical behavior of the divergence frontiers and the proposed integral summary estimated from data. We decompose the estimation error into two components, the statistical error and the quantization error, to conform with the approximation procedure commonly used in practice. We establish non-asymptotic bounds on both of the two errors. Our bounds shed light on the optimal choice of the quantization level  $k$ —they suggests that the two errors can be balanced at  $k = \Theta(n^{1/3})$ . We also derive a new concentration inequality for the frontier integral, which provides the sample complexity of achieving a small error in high probability. Finally, we demonstrate both theoretically and empirically that the use of smoothed distribution estimators can improve the estimation accuracy. All the results can be generalized to a large class of interpolation-based  $f$ -divergences. Provided theoretical results on modern data-dependent

---

<sup>1</sup><https://github.com/NVlabs/stylegan2-ada-pytorch>.

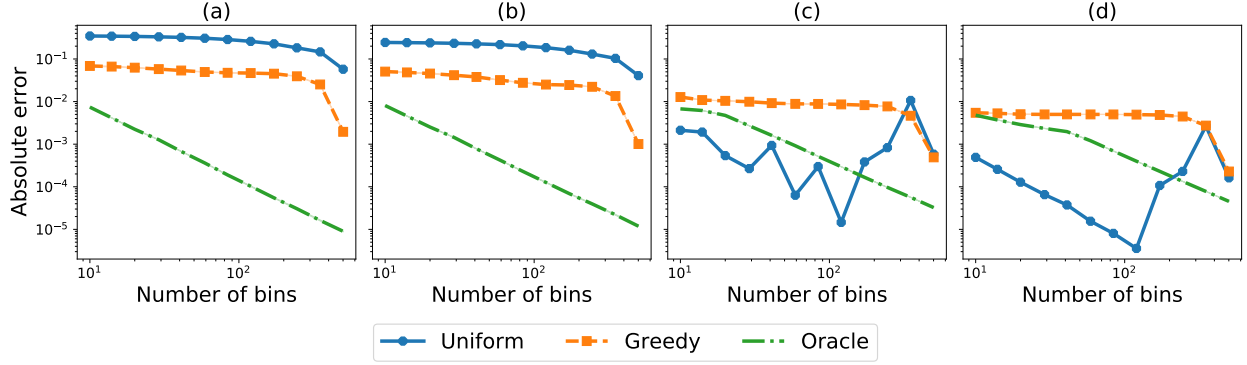


Figure 6: Absolute error versus number of bins for different quantization strategies with support size 600 (log-log scale). (a):  $\text{Dir}(1)$  and  $\text{Dir}(1/2)$ ; (b):  $\text{Zipf}(0)$  and  $\text{Dir}(1/2)$ ; (c):  $\text{Zipf}(2)$  and Step; (d):  $\text{Zipf}(1)$  and  $\text{Zipf}(2)$ .

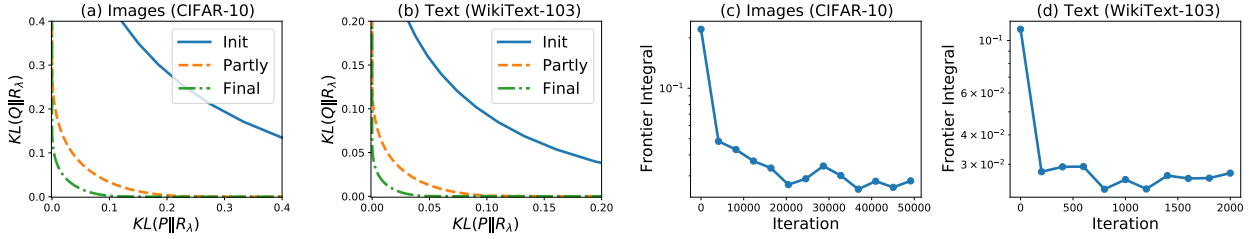


Figure 7: **Left Two:** The divergence frontier at different training checkpoints. **Right Two:** The frontier integral plotted at different training checkpoints.

quantization schemes using deep neural networks, it would be an interesting venue to specialize our bounds to such quantization schemes. Extending our results to  $\beta$ -divergences could also be interesting.

## Acknowledgments

This work was supported by NSF CCF-2019844, NSF DMS-1839371, the CIFAR program ‘‘Learning in Machines and Brains’’, and faculty research awards.

## References

- [1] M. Alamgir, G. Lugosi, and U. von Luxburg. Density-preserving quantization with application to graph downsampling. In *Conference on Learning Theory*, pages 543–559. PMLR, 2014.
- [2] D. Berend and A. Kontorovich. The missing mass problem. *Statistics & Probability Letters*, 82(6):1102–1110, 2012.
- [3] M. Binkowski, D. J. Sutherland, M. Arbel, and A. Gretton. Demystifying MMD GANs. In *ICLR*, 2018.
- [4] D. Braess and T. Sauer. Bernstein polynomials and learning theory. *J. Approx. Theory*, 128(2):187–206, 2004.
- [5] T. B. Brown, B. Mann, N. Ryder, M. Subbiah, J. Kaplan, P. Dhariwal, A. Neelakantan, P. Shyam, G. Sastry, A. Askell, S. Agarwal, A. Herbert-Voss, G. Krueger, T. Henighan, R. Child, A. Ramesh, D. M. Ziegler, J. Wu, C. Winter, C. Hesse, M. Chen, E. Sigler, M. Litwin, S. Gray, B. Chess, J. Clark, C. Berner, S. McCandlish, A. Radford, I. Sutskever, and D. Amodei. Language Models are Few-Shot Learners. In *NeurIPS*, 2020.
- [6] Y. Bu, S. Zou, Y. Liang, and V. V. Veeravalli. Estimation of KL divergence: Optimal minimax rate. *IEEE Trans. Inf. Theory*, 64(4):2648–2674, 2018.
- [7] H. Cai, S. R. Kulkarni, and S. Verdú. Universal divergence estimation for finite-alphabet sources. *IEEE Trans. Inf. Theory*, 52(8):3456–3475, 2006.
- [8] L. Chen, C. Tao, R. Zhang, R. Henao, and L. Carin. Variational Inference and Model Selection with Generalized Evidence Bounds. In *ICML*, volume 80, pages 892–901, 2018.
- [9] S. F. Chen and J. Goodman. An empirical study of smoothing techniques for language modeling. *Comput. Speech Lang.*, 13(4):359–393, 1999.
- [10] K. W. Church and W. A. Gale. A comparison of the enhanced Good-Turing and deleted estimation methods for estimating probabilities of English bigrams. *Computer Speech and Language*, 5:19–54, 1991.
- [11] I. Csiszár and P. C. Shields. Information Theory and Statistics: A Tutorial. *Found. Trends Commun. Inf. Theory*, 1(4), 2004.
- [12] P. Dhariwal, H. Jun, C. Payne, J. W. Kim, A. Radford, and I. Sutskever. Jukebox: A Generative Model for Music. *arXiv Preprint*, 2020.
- [13] A. B. Dieng, D. Tran, R. Ranganath, J. W. Paisley, and D. M. Blei. Variational Inference via  $\chi$  Upper Bound Minimization. In *NeurIPS 2017*, pages 2732–2741, 2017.
- [14] J. Djolonga, M. Lucic, M. Cuturi, O. Bachem, O. Bousquet, and S. Gelly. Precision-Recall Curves Using Information Divergence Frontiers. In *AISTATS*, pages 2550–2559, 2020.
- [15] A. Goldenshluger and O. Lepski. Structural adaptation via  $\mathbb{L}_p$ -norm oracle inequalities. *Probability Theory and Related Fields*, 143:41–71, 2009.
- [16] I. J. Good. The Population Frequencies of Species and the Estimation of Population Parameters. *Biometrika*, 40(3-4):237–264, 1953.
- [17] L. Györfi and T. Nemetz.  $f$ -dissimilarity: A generalization of the affinity of several distributions. *Annals of the Institute of Statistical Mathematics*, 30:105–113, 1978.
- [18] P. Hämäläinen, T. Saloheimo, and A. Solin. Deep residual mixture models. *arXiv preprint arXiv:2006.12063*, 2020.

- [19] Y. Han, J. Jiao, and T. Weissman. Minimax Estimation of Divergences Between Discrete Distributions. *IEEE J. Sel. Areas Inf. Theory*, 1(3):814–823, 2020.
- [20] K. He, X. Zhang, S. Ren, and J. Sun. Deep Residual Learning for Image Recognition. In *Proc. of CVPR*, pages 770–778, 2016.
- [21] A. Hegde, D. Erdogmus, T. Lehn-Schioler, Y. N. Rao, and J. C. Principe. Vector-quantization by density matching in the minimum kullback-leibler divergence sense. In *2004 IEEE International Joint Conference on Neural Networks (IEEE Cat. No. 04CH37541)*, volume 1, pages 105–109. IEEE, 2004.
- [22] M. Heusel, H. Ramsauer, T. Unterthiner, B. Nessler, and S. Hochreiter. GANs Trained by a Two Time-Scale Update Rule Converge to a Local Nash Equilibrium. In *Proc. of NeurIPS*, page 6629–6640, 2017.
- [23] D. J. Im, H. Ma, G. W. Taylor, and K. Branson. Quantitatively Evaluating GANs With Divergences Proposed for Training. In *ICLR*, 2018.
- [24] T. Karras, S. Laine, and T. Aila. A Style-Based Generator Architecture for Generative Adversarial Networks. In *CVPR*, pages 4401–4410, 2019.
- [25] T. Karras, M. Aittala, J. Hellsten, S. Laine, J. Lehtinen, and T. Aila. Training Generative Adversarial Networks with Limited Data. In *NeurIPS*, 2020.
- [26] S. M. Katz. Estimation of probabilities from sparse data for the language model component of a speech recognizer. *IEEE Trans. Acoust. Speech Signal Process.*, 35(3):400–401, 1987.
- [27] D. P. Kingma and P. Dhariwal. Glow: Generative Flow with Invertible 1x1 Convolutions. In *NeurIPS*, pages 10236–10245, 2018.
- [28] R. E. Krachevsky and V. K. Trofimov. The performance of universal encoding. *IEEE Trans. Inf. Theory*, 27(2):199–206, 1981.
- [29] A. Krizhevsky and G. Hinton. Learning Multiple Layers of Features from Tiny Images. *Technical Report*, 2009.
- [30] T. Kynkänniemi, T. Karras, S. Laine, J. Lehtinen, and T. Aila. Improved precision and recall metric for assessing generative models. In *NeurIPS*, 2019.
- [31] D. Lopez-Paz and M. Oquab. Revisiting Classifier Two-Sample Tests. In *ICLR*, 2017.
- [32] X. Mao, Q. Li, H. Xie, R. Y. K. Lau, Z. Wang, and S. P. Smolley. Least Squares Generative Adversarial Networks. In *IEEE ICCV*, pages 2813–2821, 2017.
- [33] D. Mcallester and L. Ortiz. Concentration inequalities for the missing mass and for histogram rule error. *Journal of Machine Learning Research*, 4(Oct):895–911, 2003.
- [34] D. A. McAllester and R. E. Schapire. On the convergence rate of good-turing estimators. In N. Cesa-Bianchi and S. A. Goldman, editors, *Proceedings of the Thirteenth Annual Conference on Computational Learning Theory (COLT 2000)*, June 28 - July 1, 2000, Palo Alto, California, USA, pages 1–6. Morgan Kaufmann, 2000.
- [35] S. Merity, C. Xiong, J. Bradbury, and R. Socher. Pointer Sentinel Mixture Models. In *Proc. of ICLR*, 2017.
- [36] M. F. Naeem, S. J. Oh, Y. Uh, Y. Choi, and J. Yoo. Reliable fidelity and diversity metrics for generative models. In *ICML*, volume 119, pages 7176–7185, 2020.

- [37] X. Nguyen, M. J. Wainwright, and M. I. Jordan. Estimating Divergence Functionals and the Likelihood Ratio by Convex Risk Minimization. *IEEE Trans. Inf. Theory*, 56(11):5847–5861, 2010.
- [38] F. Nielsen and R. Bhatia. *Matrix information geometry*. Springer, 2013.
- [39] A. Orlitsky and A. T. Suresh. Competitive Distribution Estimation: Why is Good-Turing Good. In *NeurIPS*, pages 2143–2151, 2015.
- [40] A. Orlitsky, N. P. Santhanam, and J. Zhang. Always good turing: Asymptotically optimal probability estimation. In *44th Symposium on Foundations of Computer Science (FOCS 2003), 11-14 October 2003, Cambridge, MA, USA, Proceedings*, pages 179–188. IEEE Computer Society, 2003.
- [41] A. Radford, J. Wu, R. Child, D. Luan, D. Amodei, and I. Sutskever. Language models are unsupervised multitask learners. *OpenAI blog*, 1(8):9, 2019.
- [42] A. Razavi, A. van den Oord, and O. Vinyals. Generating Diverse High-Fidelity Images with VQ-VAE-2. In *NeurIPS*, pages 14837–14847, 2019.
- [43] P. M. H. Ritter. Quantizing density estimators. In *NeurIPS*, volume 2, page 825. MIT Press, 2002.
- [44] P. K. Rubenstein, O. Bousquet, J. Djolonga, C. Riquelme, and I. O. Tolstikhin. Practical and Consistent Estimation of f-Divergences. In *NeurIPS*, pages 4072–4082, 2019.
- [45] A. Sablayrolles, M. Douze, C. Schmid, and H. Jégou. Spreading vectors for similarity search. In *Proc. of ICLR*, 2019.
- [46] M. S. M. Sajjadi, O. Bachem, M. Lucic, O. Bousquet, and S. Gelly. Assessing generative models via precision and recall. In *NeurIPS*, 2018.
- [47] T. Salimans, I. J. Goodfellow, W. Zaremba, V. Cheung, A. Radford, and X. Chen. Improved Techniques for Training GANs. In *NeurIPS*, pages 2226–2234, 2016.
- [48] G. R. Shorack. *Probability for Statisticians*. Springer, 2000.
- [49] J. Silva and S. Narayanan. Universal consistency of data-driven partitions for divergence estimation. In *2007 IEEE International Symposium on Information Theory*, pages 2021–2025. IEEE, 2007.
- [50] J. Silva and S. S. Narayanan. Information divergence estimation based on data-dependent partitions. *Journal of Statistical Planning and Inference*, 140(11):3180–3198, 2010.
- [51] L. Simon, R. Webster, and J. Rabin. Revisiting precision and recall definition for generative model evaluation. *CoRR*, abs/1905.05441, 2019.
- [52] C. Tao, L. Chen, R. Henao, J. Feng, and L. Carin. Chi-square Generative Adversarial Network. In *ICML*, volume 80, pages 4894–4903, 2018.
- [53] M. M. Van Hulle. Faithful representations with topographic maps. *Neural Networks*, 12(6):803–823, 1999.
- [54] S. Verdú. Empirical Estimation of Information Measures: A Literature Guide. *Entropy*, 21(8):720, 2019.
- [55] Q. Wang, S. R. Kulkarni, and S. Verdú. Divergence estimation of continuous distributions based on data-dependent partitions. *IEEE Transactions on Information Theory*, 51(9):3064–3074, 2005.
- [56] Y. Wang, D. Ramanan, and M. Hebert. Learning to Model the Tail. In *NeurIPS*, pages 7029–7039, 2017.
- [57] T. Wolf, L. Debut, V. Sanh, J. Chaumond, C. Delangue, A. Moi, P. Cistac, T. Rault, R. Louf, M. Funtowicz, J. Davison, S. Shleifer, P. von Platen, C. Ma, Y. Jernite, J. Plu, C. Xu, T. L. Scao, S. Gugger, M. Drame, Q. Lhoest, and A. M. Rush. Transformers: State-of-the-Art Natural Language Processing. In *Proc. of EMNLP*, pages 38–45, 10 2020.

- [58] R. Zellers, A. Holtzman, H. Rashkin, Y. Bisk, A. Farhadi, F. Roesner, and Y. Choi. Defending Against Neural Fake News. In *NeurIPS*, 2019.
- [59] Z. Zhang and M. Grabchak. Nonparametric estimation of Kullback-Leibler divergence. *Neural Comput.*, 26(11):2570–2593, 2014.

# Appendix

## Table of Contents

---

<b>A</b>	<i>f</i> -divergence: review and examples	18
<b>B</b>	Properties of the frontier integral	19
<b>C</b>	Regularity assumptions	20
C.1	Assumptions	20
C.2	Examples satisfying the assumptions	21
C.3	Properties and useful lemmas	23
<b>D</b>	Plug-in estimator	25
D.1	Statistical error	26
D.2	Concentration bound	28
<b>E</b>	Add-constant smoothing	30
<b>F</b>	Quantization error	32
<b>G</b>	Experimental details	34
G.1	Synthetic data	34
G.2	Real data	38
<b>H</b>	Length of the divergence frontier	40
<b>I</b>	Technical lemmas	42

---

## A $f$ -divergence: review and examples

We review the definition of  $f$ -divergences and give a few examples.

Let  $f : (0, \infty) \rightarrow \mathbb{R}$  be a convex function with  $f(1) = 0$ . Let  $P, Q \in \mathcal{P}(\mathcal{X})$  be dominated by some measure  $\mu \in \mathcal{P}(\mathcal{X})$  with densities  $p$  and  $q$ , respectively. The  $f$ -divergence generated by  $f$  is

$$D_f(P\|Q) = \int_{\mathcal{X}} q(x) f\left(\frac{p(x)}{q(x)}\right) d\mu(x),$$

with the convention that  $f(0) := \lim_{t \rightarrow 0^+} f(t)$  and  $0f(p/0) = pf^*(0)$ , where  $f^*(0) = \lim_{x \rightarrow 0^+} xf(1/x) \in [0, \infty]$ . Hence,  $D_f(P\|Q)$  can be rewritten as

$$D_f(P\|Q) = \int_{q>0} q(x) f\left(\frac{p(x)}{q(x)}\right) d\mu(x) + f^*(0)P[q=0],$$

with the agreement that the last term is zero if  $P[q=0] = 0$  no matter what value  $f^*(0)$  takes (which could be infinity). For any  $c \in \mathbb{R}$ , it holds that  $D_{f_c}(P\|Q) = D_f(P\|Q)$  where  $f_c(t) = f(t) + c(t-1)$ . Hence, we also assume, w.l.o.g., that  $f(t) \geq 0$  for all  $t \in (0, \infty)$ . To summarize,  $f$  is convex and nonnegative with  $f(1) = 0$ . As a result,  $f$  is non-increasing on  $(0, 1]$  and non-decreasing on  $[1, \infty)$ .

The conjugate generator to  $f$  is the function  $f^* : (0, \infty) \rightarrow [0, \infty)$  defined by<sup>2</sup>

$$f^*(t) = tf(1/t),$$

where again we define  $f^*(0) = \lim_{t \rightarrow 0^+} f^*(t)$ . Since  $f^*$  can be constructed by the perspective transform of  $f$ , it is also convex. We can verify that  $f^*(1) = 0$  and  $f^*(t) \geq 0$  for all  $t \in (0, \infty)$ , so it defines another divergence  $D_{f^*}$ . We call this the *conjugate divergence* to  $D_f$  since

$$D_{f^*}(P\|Q) = D_f(Q\|P).$$

The divergence  $D_f$  is symmetric if and only if  $f = f^*$ , and we write it as  $D_f(P, Q)$  to emphasize the symmetry.

**Example 5.** We illustrate a number of examples.

- (a) KL divergence: It is an  $f$ -divergence generated by  $f_{\text{KL}}(t) = t \log t - t + 1$ .
- (b) Interpolated KL divergence: For  $\lambda \in (0, 1)$ , the interpolated KL divergence is defined as

$$\text{KL}_\lambda(P\|Q) = \text{KL}(P\|\lambda P + (1-\lambda)Q),$$

which is a  $f$ -divergence generated by

$$f_{\text{KL},\lambda}(t) = t \log\left(\frac{t}{\lambda t + 1 - \lambda}\right) - (1-\lambda)(t-1).$$

- (c) Jensen-Shannon divergence: The Jensen-Shannon Divergence is defined as

$$D_{\text{JS}}(P, Q) = \frac{1}{2}\text{KL}_{1/2}(P\|Q) + \frac{1}{2}\text{KL}_{1/2}(Q\|P).$$

More generally, we have the  $\lambda$ -skew Jensen-Shannon Divergence [38], which is defined for  $\lambda \in (0, 1)$  as  $D_{\text{JS},\lambda} = \lambda \text{KL}_\lambda(P\|Q) + (1-\lambda)\text{KL}_{1-\lambda}(Q\|P)$ . This is an  $f$ -divergence generated by

$$f_{\text{JS},\lambda}(t) = \lambda t \log\left(\frac{t}{\lambda t + 1 - \lambda}\right) + (1-\lambda) \log\left(\frac{1}{\lambda t + 1 - \lambda}\right).$$

<sup>2</sup>The conjugacy between  $f$  and  $f^*$  is unrelated to the usual Fenchel or Lagrange duality in convex analysis, but is related to the perspective transform.

(d) Frontier Integral: From Proposition 6, FI is an  $f$ -divergence generated by

$$f_{\text{FI}}(t) = \frac{t+1}{2} - \frac{t}{t-1} \log t.$$

(e) Interpolated  $\chi^2$  divergence: Similar to the interpolated KL divergence, we can define the interpolated  $\chi^2$  divergence  $D_{\chi^2, \lambda}$  and the corresponding convex generator  $f_{\chi^2, \lambda}$  for  $\lambda \in (0, 1)$  as

$$D_{\chi^2, \lambda}(P\|Q) = D_{\chi^2}(P\|\lambda P + (1-\lambda)Q), \quad \text{and,} \quad f_{\chi^2, \lambda}(t) = \frac{(t-1)^2}{\lambda t + 1 - \lambda}.$$

The usual Neyman and Pearson  $\chi^2$  divergences are respectively obtained in the limits  $\lambda \rightarrow 1$  and  $\lambda \rightarrow 0$ .

(f) Squared Le Cam distance: The squared Le Cam distance is, up to scaling, a special case of the interpolated  $\chi^2$  divergence with  $\lambda = 1/2$ :

$$D_{\text{LC}}(P, Q) = \frac{1}{4} D_{\chi^2, 1/2}(P\|Q).$$

(g) Squared Hellinger Distance: It is an  $f$ -divergence generated by  $f_H(t) = (1 - \sqrt{t})^2$ .

## B Properties of the frontier integral

We prove some properties of the frontier integral here. First, the frontier integral can be computed in closed form as below.

**Proposition 6.** *Let  $P$  and  $Q$  be dominated by some probability measure  $\mu$  with density  $p$  and  $q$ , respectively. Then,*

$$\text{FI}(P, Q) = \int_{\mathcal{X}} \mathbb{1}\{p(x) \neq q(x)\} \left( \frac{p(x) + q(x)}{2} - \frac{p(x)q(x)}{p(x) - q(x)} \log \frac{p(x)}{q(x)} \right) d\mu(x), \quad (9)$$

with the convention  $0 \log 0 = 0$ . Moreover, FI is an  $f$ -divergence generated by the convex function

$$f_{\text{FI}}(t) = \frac{t+1}{2} - \frac{t}{t-1} \log t,$$

with the understanding that  $f_{\text{FI}}(1) = \lim_{t \rightarrow 1} f_{\text{FI}}(t) = 0$ .

*Proof of Proposition 6.* Let  $\bar{\lambda} = 1 - \lambda$ . By Tonelli's theorem, it holds that  $\text{FI}(P, Q) = 2 \int_{\mathcal{X}} h(p(x), q(x)) d\mu(x)$ , where

$$h(p, q) = \int_0^1 (\lambda p \log p + \bar{\lambda} q \log q - (\lambda p + \bar{\lambda} q) \log(\lambda p + \bar{\lambda} q)) d\lambda.$$

When  $p = q$ , the integrand is 0. If  $q = 0$ , then the second term inside the integral is 0, while the first term is

$$\int_0^1 \lambda p \log \frac{1}{\lambda} d\lambda = \frac{p}{4}.$$

Finally, when  $p \neq q$  are both non-zero, we evaluate the integral to get,

$$h(p, q) = \frac{p}{2} \log p + \frac{q}{2} \log q - \frac{2p^2 \log p - p^2 - 2q^2 \log q + q^2}{4(p-q)},$$

and rearranging the expression completes the proof.  $\square$

Next, the frontier integral is symmetric and bounded.

**Proposition 7.** *The frontier integral satisfies the following properties:*

- (a)  $\text{FI}(P, Q) = \text{FI}(Q, P)$ .
- (b)  $0 \leq \text{FI}(P, Q) \leq 1$  with  $\text{FI}(P, Q) = 0$  if and only if  $P = Q$ .

*Proof of Proposition 7.* The first part follows from the closed form expression in Proposition 6. For the second part, we get the upper bound as

$$\text{FI}(P, Q) \leq \int_{\mathcal{X}} \frac{p(x) + q(x)}{2} d\mu(x) = 1.$$

We have  $\text{FI}(P, Q) \geq 0$  with  $\text{FI}(P, P) = 0$  since  $\text{FI}$  is an  $f$ -divergence. Using properties of  $f$ -divergences, we get that  $\text{FI}(P, Q) = 0$  only if  $P = Q$ , since  $f_{\text{FI}}$  is strictly convex at 1 [e.g., 11, Lemma 4.1].  $\square$

At first glance, it appears that the frontier integral might be related to the length of the divergence frontier, but this is not so. We show in Appendix H that the latter can be unbounded while Proposition 7 shows that the former always lies in  $[0, 1]$ .

## C Regularity assumptions

In this section, we state and discuss the regularity assumptions required for the statistical error bounds. Throughout, we assume that  $\mathcal{X}$  is a finite set (for instance, on the quantized space). We upper bound the expected error of the empirical  $f$ -divergences estimated from data.

We use the convention that all higher order derivatives of  $f$  and  $f^*$  at 0 are defined as the corresponding limits as  $x \rightarrow 0^+$  (if they exist). Further, we use the notation

$$\psi(p, q) = qf(p/q) = pf^*(q/p), \quad (10)$$

so that  $D_f(P\|Q) = \sum_{a \in \mathcal{X}} \psi(P(a), Q(a))$ .

### C.1 Assumptions

We make the following assumptions about the functions  $f$  and  $f^*$ .

**Assumption 8.** The generator  $f$  is twice continuously differentiable with  $f'(1) = 0$ . Moreover,

- (A1) We have  $C_0 := f(0) < \infty$  and  $C_0^* := f^*(0) < \infty$ .
- (A2) There exist constants  $C_1, C_1^* < \infty$  such that for every  $x \in (0, 1)$ , we have,

$$|f'(t)| \leq C_1 (1 \vee \log 1/t), \quad \text{and,} \quad |(f^*)'(t)| \leq C_1^* (1 \vee \log 1/t).$$

- (A3) There exist constants  $C_2, C_2^* < \infty$  such that for every  $t \in (0, \infty)$ , we have,

$$\frac{t}{2} f''(t) \leq C_2, \quad \text{and,} \quad \frac{t}{2} (f^*)''(t) \leq C_2^*.$$

**Remark 9.** We discuss the asymptotics of the assumptions.

- (a) Assumption (A1) ensures boundedness of the  $f$ -divergence. Indeed,  $f(0) = \infty$  leads to  $D_f(P\|Q) = \infty$  if there exists an atom  $a \in \mathcal{X}$  such that  $P(a) = 0$  but  $Q(a) \neq 0$ . This happens, for instance, with the reverse KL divergence ( $f(t) = -\log t + t - 1$ ). By symmetry,  $f^*(0) = \infty$  leads to a case where  $D_f(P\|Q) = \infty$  if there exists an atom  $a \in \mathcal{X}$  such that  $Q(a) = 0$  but  $P(a) \neq 0$ , as in the (forward) KL divergence.
- (b) Since  $f'$  is monotonic nondecreasing and  $f'(1) = 0$ , we have that  $f'(0) \leq 0$  (with strict inequality if  $f$  is strictly convex at 1). In fact,  $f'(0) = -\infty$  for each of the divergences considered in Example 5. Assumption (A2) requires  $f'(t)$  to behave as  $\log 1/t$  when  $t \rightarrow 0$ . Likewise for  $(f^*)'$ .

Table 1: Examples of  $f$ -divergences and whether they satisfy Assumptions **(A1)-(A3)**. Here,  $\lambda \in (0, 1)$  is a parameter of the interpolated or skew divergences, and we define  $\bar{\lambda} := 1 - \lambda$ .

$f$ -divergence	Satisfies Assumptions?	$C_0$	$C_0^*$	$C_1$	$C_1^*$	$C_2$	$C_2^*$
KL	No	1	$\infty$				
Interpolated KL	Yes	$\bar{\lambda}$	$\log \frac{1}{\bar{\lambda}} - \bar{\lambda}$	1	$\frac{\bar{\lambda}^2}{\lambda}$	$\frac{1}{2}$	$\frac{\bar{\lambda}}{8\lambda}$
JS	Yes	$\frac{1}{2} \log 2$	$\frac{1}{2} \log 2$	$\frac{1}{2}$	$\frac{1}{2}$	$\frac{1}{4}$	$\frac{1}{4}$
Skew JS	Yes	$\bar{\lambda} \log \frac{1}{\bar{\lambda}}$	$\lambda \log \frac{1}{\lambda}$	$\lambda$	$\bar{\lambda}$	$\frac{\lambda}{2}$	$\frac{\bar{\lambda}}{2}$
Frontier integral	Yes	$\frac{1}{2}$	$\frac{1}{2}$	4	4	$\frac{1}{2}$	$\frac{1}{2}$
LeCam	Yes	$\frac{1}{2}$	$\frac{1}{2}$	2	2	$\frac{8}{27}$	$\frac{8}{27}$
Interpolated $\chi^2$	Yes	$\frac{1}{\lambda}$	$\frac{1}{\bar{\lambda}}$	$\frac{2}{\bar{\lambda}^2}$	$\frac{2}{\lambda^2}$	$\frac{4}{27\lambda\bar{\lambda}^2}$	$\frac{4}{27\lambda^2\bar{\lambda}}$
Hellinger	No	1	1	$\infty$	$\infty$		

- (c) Likewise, we have that  $f''(0) = \infty$  and  $f''(\infty) = 0$  for each of the divergence considered in Example 5. However, Assumption **(A3)** makes assumptions on the rates of these limits. Namely,  $f''$  should diverge no faster than  $1/t$  as  $t \rightarrow 0$  and  $f''$  should converge to 0 at least as fast as  $1/t^2$  as  $t \rightarrow \infty$ . We can summarize the implied asymptotics of  $f''$  as

$$f''(t) = \begin{cases} \Omega(1/t), & \text{if } t \rightarrow 0, \\ O(1/t^2), & \text{if } t \rightarrow \infty. \end{cases}$$

## C.2 Examples satisfying the assumptions

We now consider the examples in Example 5. The constants are summarized in Table 1.

**KL divergence.** We have

$$f_{\text{KL}}(t) = t \log t - t + 1 \quad \text{and} \quad f_{\text{KL}}^*(t) = -\log t + t - 1.$$

We have  $f(0) = 1$  but  $f^*(0) = \infty$ . Therefore, the KL divergence does not satisfy our assumptions. Indeed, this is because the KL divergence can be unbounded [6].

**Interpolated KL Divergence.** Let  $\lambda \in (0, 1)$  be a parameter and denote  $\bar{\lambda} = 1 - \lambda$ . We have

$$f_{\text{KL},\lambda}(t) = t \log \left( \frac{t}{\lambda t + \bar{\lambda}} \right) - \bar{\lambda}(t - 1) \quad \text{and} \quad f_{\text{KL},\lambda}^*(t) = -\log(\bar{\lambda}t + \lambda) + \bar{\lambda}(t - 1).$$

The corresponding derivatives are

$$\begin{aligned} f'_{\text{KL},\lambda}(t) &= \frac{\bar{\lambda}}{\lambda t + \bar{\lambda}} + \log \left( \frac{t}{\lambda t + \bar{\lambda}} \right) - \bar{\lambda}, & (f_{\text{KL},\lambda}^*)'(t) &= \bar{\lambda} - \frac{\bar{\lambda}}{\lambda t + \bar{\lambda}}, \\ f''_{\text{KL},\lambda}(t) &= \frac{\bar{\lambda}^2}{t(\lambda t + \bar{\lambda})^2}, & (f_{\text{KL},\lambda}^*)''(t) &= \frac{\bar{\lambda}^2}{(\lambda t + \bar{\lambda})^2}. \end{aligned}$$

**Proposition 10.** *The interpolated KL divergence generated by  $f_{\text{KL},\lambda}$  satisfies Assumption 8 with*

$$C_0 = 1 - \lambda, \quad C_0^* = \log \frac{1}{\lambda} - 1 + \lambda, \quad C_1 = 1, \quad C_1^* = \frac{(1 - \lambda)^2}{\lambda}, \quad C_2 = \frac{1}{2}, \quad C_2^* = \frac{1 - \lambda}{8\lambda}.$$

*Proof.* First,  $C_0, C_0^*$  can be computed directly. Second, it is clear that

$$-f'_{\text{KL},\lambda}(t) = \log \frac{1}{t} + \log(\lambda t + \bar{\lambda}) - \frac{\bar{\lambda}}{\lambda t + \bar{\lambda}} + \bar{\lambda} \leq \log \frac{1}{t} + \log 1 - \bar{\lambda} + \bar{\lambda} = \log \frac{1}{t}$$

for all  $x \in (0, 1)$ . Moreover, since  $f$  is convex and  $f'_{\text{KL},\lambda}(1) = 0$ , it holds that  $f'_{\text{KL},\lambda}(x) \leq 0$  for all  $x \in (0, 1)$ , and thus  $C_1 = 1$ . Next, we note that  $|(f_{\text{KL},\lambda}^*)'(x)| \leq \bar{\lambda}^2/\lambda$  holds uniformly on  $(0, 1)$  (or equivalently that  $f_{\text{KL},\lambda}^*$  is Lipschitz); this gives  $C_1^*$ . Next, we have

$$C_2 = \sup_{t>0} \left\{ \frac{1}{2} t f''_{\text{KL},\lambda}(t) \right\} \leq \frac{1}{2},$$

since the function inside the sup is monotonic decreasing on  $(0, \infty)$ . Finally, we have

$$C_2^* = \sup_{t>0} \left\{ \frac{1}{2} t (f_{\text{KL},\lambda}^*)''(t) \right\} = \frac{\bar{\lambda}}{8\lambda},$$

since the term inside the sup is maximized at  $t = \lambda/\bar{\lambda}$ .  $\square$

**Skew Jensen-Shannon Divergence.** Let  $\lambda \in (0, 1)$  be a parameter and  $\bar{\lambda} = 1 - \lambda$ . We have,

$$f_{\text{JS},\lambda}(t) = \lambda t \log \left( \frac{t}{\lambda t + \bar{\lambda}} \right) + \bar{\lambda} \log \left( \frac{1}{\lambda t + \bar{\lambda}} \right) = f_{\text{JS},1-\lambda}^*(t).$$

Its derivatives are

$$f'_{\text{JS},\lambda}(t) = \lambda \log \left( \frac{t}{\lambda t + \bar{\lambda}} \right) \quad \text{and} \quad f''_{\text{JS},\lambda}(t) = \frac{\lambda \bar{\lambda}}{t(\lambda t + \bar{\lambda})}.$$

**Proposition 11.** *The skew JS divergence generated by  $f_{\text{JS},\lambda}$  above satisfies Assumption 8 with*

$$C_0 = (1 - \lambda) \log \frac{1}{1 - \lambda}, \quad C_0^* = \lambda \log \frac{1}{\lambda}, \quad C_1 = \lambda, \quad C_1^* = 1 - \lambda, \quad C_2 = \frac{\lambda}{2}, \quad C_2^* = \frac{1 - \lambda}{2}.$$

*Proof.* For  $C_1$ , we have

$$-f'_{\text{JS},\lambda}(t) = \lambda \log \frac{1}{t} + \lambda \log(\lambda t + \bar{\lambda}) \leq \lambda \log \frac{1}{t}$$

for  $x \in (0, 1)$ . Next, we have

$$C_2 = \frac{\lambda \bar{\lambda}}{2} \sup_{t>0} \frac{1}{\lambda t + \bar{\lambda}} = \frac{\lambda}{2}.$$

$\square$

**Frontier integral.** We have

$$f_{\text{FI}}(t) = \frac{t+1}{2} - \frac{t}{t-1} \log t = f_{\text{FI}}^*(t).$$

Its derivatives are

$$f'_{\text{FI}}(t) = \frac{(1-t)(3-t) + 2 \log t}{2(1-t)^2} \quad \text{and} \quad f''_{\text{FI}}(t) = \frac{2t \log t - t^2 + 1}{t(1-t)^3}.$$

**Proposition 12.** *The frontier integral satisfies Assumption 8 with*

$$C_0 = \frac{1}{2} = C_0^*, \quad C_1 = 1 = C_1^*, \quad C_2 = \frac{1}{2} = C_2^*.$$

*Proof.* We get  $C_0$  by calculating the limit as  $x \rightarrow 0$  using L'Hôpital's rule. For  $C_2$ , we note that the term inside the sup below is decreasing in  $x$  to get

$$C_2 = \sup_{t>0} \frac{2t \log t - t^2 + 1}{(1-t)^3} = \frac{1}{2}.$$

By definition,

$$f_{\text{FI}}(t) = 2 \int_0^1 f_{\text{JS},\lambda}(t) d\lambda,$$

so that, by Proposition 11,

$$-f'_{\text{FI}}(t) = -2 \int_0^1 f'_{\text{JS},\lambda}(t) d\lambda \leq 2 \int_0^1 \lambda \log \frac{1}{t} d\lambda = \log \frac{1}{t}.$$

□

**Interpolated  $\chi^2$  divergence.** Let  $\lambda \in (0, 1)$  be a parameter and denote  $\bar{\lambda} = 1 - \lambda$ . We have,

$$f_{\chi^2,\lambda}(t) = \frac{(t-1)^2}{\lambda t + 1 - \lambda} = f_{\chi^2,1-\lambda}^*(t).$$

Its derivatives are

$$f'_{\chi^2,\lambda}(t) = \frac{(t-1)(\lambda t + \bar{\lambda} + 1)}{(\lambda t + \bar{\lambda})^2} \quad \text{and} \quad f''_{\chi^2,\lambda}(t) = \frac{2}{(\lambda t + \bar{\lambda})^2}.$$

**Proposition 13.** For  $\lambda \in (0, 1)$ , the interpolated  $\chi^2$ -divergence satisfies Assumption 8 with

$$\begin{aligned} C_0 &= \frac{1}{1-\lambda}, & C_0^* &= \frac{1}{\lambda}, & C_1 &= \frac{2}{(1-\lambda)^2}, & C_1^* &= \frac{2}{\lambda^2} \\ C_2 &= \frac{4}{27\lambda(1-\lambda)^2}, & C_2^* &= \frac{4}{27\lambda^2(1-\lambda)}. \end{aligned}$$

*Proof.* Note that  $0 \geq f'_{\chi^2,\lambda}(0) = -(1 + \bar{\lambda})/\bar{\lambda}^2 \geq -2/\bar{\lambda}^2$  is bounded. Since  $f'_{\chi^2,\lambda}$  is monotonic increasing with  $f'_{\chi^2,\lambda}(1) = 0$ , this gives the bound on  $C_1$ . Next, we bound

$$C_2 = \sup_{t>0} \frac{t}{(\lambda t + \bar{\lambda})^3} = \frac{4}{27\lambda\bar{\lambda}^2},$$

since the supremum is attained at  $t = \bar{\lambda}/(2\lambda)$ . □

**Squared Hellinger distance.** We have,

$$f_H(t) = (1 - \sqrt{t})^2 = f_H^*(t), \quad f'_H(t) = 1 - \frac{1}{\sqrt{t}}, \quad f''_H(t) = \frac{1}{2}t^{-3/2}.$$

The squared Hellinger divergence does not satisfy our assumptions since for  $t < 1$ ,  $|f'_H(x)| \approx 1/\sqrt{t}$  diverges faster than the  $\log 1/t$  rate required by Assumption (A2).

### C.3 Properties and useful lemmas

We state here some useful properties and lemmas that we use throughout the paper.

First, we express the derivatives of  $\psi(p, q) = qf(p/q)$  in terms of the derivatives of  $f$ :

$$\frac{\partial \psi}{\partial p}(p, q) = f' \left( \frac{p}{q} \right) = f^* \left( \frac{q}{p} \right) - \frac{q}{p} (f^*)' \left( \frac{q}{p} \right) \quad (11a)$$

$$\frac{\partial \psi}{\partial q}(p, q) = f \left( \frac{p}{q} \right) - \frac{p}{q} f' \left( \frac{p}{q} \right) = (f^*)' \left( \frac{q}{p} \right) \quad (11b)$$

$$\frac{\partial^2 \psi}{\partial p^2}(p, q) = \frac{1}{q} f'' \left( \frac{p}{q} \right) = \frac{q^2}{p^3} (f^*)'' \left( \frac{q}{p} \right) \geq 0 \quad (11c)$$

$$\frac{\partial^2 \psi}{\partial q^2}(p, q) = \frac{p^2}{q^3} f'' \left( \frac{p}{q} \right) = \frac{1}{p} (f^*)'' \left( \frac{q}{p} \right) \geq 0 \quad (11d)$$

$$\frac{\partial^2 \psi}{\partial p \partial q}(p, q) = -\frac{p}{q^2} f'' \left( \frac{p}{q} \right) = -\frac{q}{p^2} (f^*)'' \left( \frac{q}{p} \right) \leq 0, \quad (11e)$$

where the inequalities  $f'', (f^*)'' \geq 0$  followed from convexity of  $f$  and  $f^*$  respectively.

The next lemma shows that the function  $\psi$  is nearly Lipschitz, up to a log factor. This is the generalization of the approximate Lipschitz lemma in Lemma 2 to the case of general  $f$ -divergences. This lemma can be leveraged to directly obtain a bound on statistical error of the  $f$ -divergence in terms of the expected total variation distance, provided the probabilities are not too small.

**Lemma 14.** *Suppose that  $f$  satisfies Assumption 8. Consider  $\psi : [0, 1] \times [0, 1] \rightarrow [0, \infty)$  given by  $\psi(p, q) = qf(p/q)$ . We have, for all  $p, p', q, q' \in [0, 1]$  with  $p \vee p' > 0, q \vee q' > 0$ , that*

$$\begin{aligned} |\psi(p', q) - \psi(p, q)| &\leq \left( C_1 \max \left\{ 1, \log \frac{1}{p \vee p'} \right\} + C_0^* \vee C_2 \right) |p - p'| \\ |\psi(p, q') - \psi(p, q)| &\leq \left( C_1^* \max \left\{ 1, \log \frac{1}{q \vee q'} \right\} + C_0 \vee C_2^* \right) |q - q'|. \end{aligned}$$

*Proof.* We only prove the first inequality. The second one is identical with the use of  $f^*$  rather than  $f$ . Suppose  $p' \geq p$ . From the fact that  $\psi$  is convex in  $p$  together with a Taylor expansion of  $\psi(\cdot, q)$  around  $p'$ , we get,

$$\begin{aligned} 0 \leq \psi(p, q) - \psi(p', q) - (p - p') \frac{\partial \psi}{\partial p}(p', q) &= \frac{1}{2} \int_{p'}^p \frac{\partial^2 \psi}{\partial p^2}(s, q)(p - s) ds \\ &= -\frac{p}{2} \int_p^{p'} \frac{\partial^2 \psi}{\partial p^2}(s, q) ds + \frac{1}{2} \int_p^{p'} s \frac{\partial^2 \psi}{\partial p^2}(s, q) ds \\ &\leq 0 + C_2(p' - p), \end{aligned}$$

where we used  $\partial^2 \psi / \partial p^2$  is non-negative due to convexity and, by (11c) and Assumption (A3),

$$s \frac{\partial^2 \psi}{\partial p^2}(s, q) = \frac{s}{q} f''(s/q) \leq 2C_2.$$

This yields

$$-(p' - p) \frac{\partial \psi}{\partial p}(p', q) \leq \psi(p, q) - \psi(p', q) \leq -(p' - p) \frac{\partial \psi}{\partial p}(p', q) + C_2(p' - p).$$

We consider two cases based on the sign of  $\frac{\partial \psi}{\partial p}(p', q) = f'(p/q)$  (cf. Eq. (11e)).

**Case 1.**  $\frac{\partial \psi}{\partial p}(p', q) \geq 0$ . Since  $q \mapsto f'(p/q)$  is decreasing in  $q$ , we have

$$0 \leq (p' - p) \frac{\partial \psi}{\partial p}(p', q) = (p' - p) f'(p/q) \leq \lim_{q \rightarrow 0} (p' - p) f'(p/q) = (p' - p) f^*(0),$$

where we used  $f'(\infty) = f^*(0)$  from Lemma 15. From Assumption (A1), we get the bound

$$|\psi(p, q) - \psi(p', q)| \leq (C_0^* \vee C_2)(p' - p).$$

**Case 2.**  $\frac{\partial \psi}{\partial p}(p', q) < 0$ . By Assumption (A2), it holds that

$$\left| \frac{\partial \psi}{\partial p}(p', q) \right| \leq C_1 \max\{1, \log(q/p')\} \leq C_1 \max\{1, \log(1/p')\},$$

and thus

$$|\psi(p, q) - \psi(p', q)| \leq \left( C_1 \max\left\{1, \log \frac{1}{p'}\right\} + C_2 \right) (p' - p).$$

□

With the above lemma, the estimation error of the empirical  $f$ -divergence can be upper bounded by the total variation distance between the empirical measure and its population counterpart up to a logarithmic factor, where:

$$\|\hat{P}_n - P\|_{\text{TV}} = \sum_{a \in \mathcal{X}} |\hat{P}_n(a) - P(a)|. \quad (12)$$

Next, we state and prove a technical lemma.

**Lemma 15.** *Suppose the generator  $f$  satisfies Assumptions (A1) and (A2). Then,*

$$\lim_{t \rightarrow \infty} f'(t) = f^*(0), \quad \text{and} \quad \lim_{t \rightarrow \infty} (f^*)'(t) = f(0).$$

*Proof.* We start by observing that

$$\lim_{t \rightarrow 0} t|f'(t)| \leq C_1 \lim_{t \rightarrow 0} t \vee t \log \frac{1}{t} = 0.$$

Next, a direct calculation gives

$$(f^*)'(1/t) = f(t) - tf'(t),$$

so that taking the limit  $t \rightarrow 0$  gives

$$\lim_{t \rightarrow \infty} (f^*)'(t) = f(0) - \lim_{t \rightarrow 0} tf'(t) = f(0).$$

The proof of the other part is identical. □

## D Plug-in estimator

In this section, we prove the high probability concentration bound for the plug-in estimator. There are two key steps: bounding the statistical error and giving a deviation bound.

Throughout this section, we assume that  $P$  and  $Q$  are discrete. Let  $\{X_i\}_{i=1}^n$  and  $\{Y_j\}_{j=1}^m$  be two independent i.i.d. samples from  $P$  and  $Q$ , respectively. We consider the plug-in estimator of the  $f$ -divergences, i.e.,  $D_f(\hat{P}_n \parallel \hat{Q}_m)$ . The main results are (a) an upper bound for its statistical error, and (b) a high probability concentration bound.

## D.1 Statistical error

**Proposition 16.** Suppose that  $f$  satisfies Assumption 8 and  $k := |\text{Supp}(P)| \vee |\text{Supp}(Q)| \in \mathbb{N} \cup \{\infty\}$ . Let  $n, m \geq 3$ . Let  $c_1 = C_1 + C_1^*$  and  $c_2 = C_2 \vee C_2^* + C_2^* \vee C_0$ . We have,

$$\begin{aligned} \mathbb{E}|D_f(P\|Q) - D_f(\hat{P}_n\|\hat{Q}_m)| &\leq (C_1 \log n + C_0^* \vee C_2) \alpha_n(P) + (C_1^* \log m + C_0 \vee C_2^*) \alpha_m(Q) \\ &\quad + (C_1 + C_0^* \vee C_2) \beta_n(P) + (C_1^* + C_0 \vee C_2^*) \beta_m(Q), \end{aligned} \quad (13)$$

where  $\alpha_n(P) = \sum_{a \in \mathcal{X}} \sqrt{n^{-1}P(a)}$  and  $\beta_n(P) = \mathbb{E}[\sum_{a:\hat{P}_n(a)=0} P(a) \max\{1, \log(1/P(a))\}]$ . Furthermore, if  $k < \infty$ , then

$$\mathbb{E}|D_f(P\|Q) - D_f(\hat{P}_n\|\hat{Q}_m)| \leq (c_1 \log(n \wedge m) + c_2) \left( \sqrt{\frac{k}{n \wedge m}} + \frac{k}{n \wedge m} \right). \quad (14)$$

The proof relies on two key lemmas—the approximate Lipschitz lemma (Lemma 14) and the missing mass lemma (Lemma 18). The argument breaks into two cases in  $P$  (and analogously for  $Q$ ) for each atom  $a \in \mathcal{X}$ :

- (a)  $\hat{P}_n(a) > 0$ : Since  $\hat{P}_n$  is an empirical measure, we have that  $\hat{P}_n(a) \geq 1/n$ . In this case the approximate Lipschitz lemma gives us the Lipschitzness in  $\|P - \hat{P}_n\|_{\text{TV}}$  up to a factor of  $\log n$ .
- (b)  $\hat{P}_n(a) = 0$ : In this case, the mass corresponding to  $P(a)$  is missing in the empirical measure and we directly bound its expectation following similar arguments as in the missing mass literature; see, e.g., [2, 33].

For the first part, we further upper bound the expected total variation distance of the plug-in estimator, which is

$$\|\hat{P}_n - P\|_{\text{TV}} = \sum_{a \in \mathcal{X}} |\hat{P}_n(a) - P(a)|.$$

**Lemma 17.** Assume that  $P$  is discrete. For any  $n \geq 1$ , it holds that

$$\mathbb{E}\|\hat{P}_n - P\|_{\text{TV}} \leq \alpha_n(P).$$

Furthermore, if  $k = |\text{Supp}(P)| < \infty$ , then

$$\mathbb{E}\|\hat{P}_n - P\|_{\text{TV}} \leq \alpha_n(P) \leq \sqrt{\frac{k}{n}}.$$

*Proof.* Using Jensen's inequality, we have,

$$\begin{aligned} \mathbb{E} \sum_{a \in \text{Supp}(P)} |\hat{P}_n(a) - P(a)| &\leq \sum_{a \in \text{Supp}(P)} \sqrt{\mathbb{E}(\hat{P}_n(a) - P(a))^2} \\ &= \sum_{a \in \text{Supp}(P)} \sqrt{\frac{P(a)(1 - P(a))}{n}} \leq \alpha_n(P), \end{aligned}$$

If  $k < \infty$ , then it follows from Jensen's inequality applied to the concave function  $t \mapsto \sqrt{t}$  that

$$\frac{1}{k} \sum_{i=1}^k \sqrt{a_k} \leq \sqrt{\frac{1}{k} \sum_{i=1}^k a_k}.$$

Hence,  $\alpha_n(P) \leq k/n$  and it completes the proof.  $\square$

For the second part, we treat the missing mass directly.

**Lemma 18** (Missing Mass). *Assume that  $k = |\text{Supp}(P)| < \infty$ . Then, for any  $n \geq 3$ ,*

$$\mathbb{E} \left[ \sum_{a \in \mathcal{X}} \mathbb{1}\{\hat{P}_n(a) = 0\} P(a) \right] \leq \frac{k}{n} \quad (15)$$

$$\beta_n(P) := \mathbb{E} \left[ \sum_{a \in \mathcal{X}} \mathbb{1}\{\hat{P}_n(a) = 0\} P(a) \left( 1 \vee \log \frac{1}{P(a)} \right) \right] \leq \frac{k \log n}{n}, \quad (16)$$

where  $a \vee b := \max\{a, b\}$ .

*Proof.* We prove the second inequality. The first one is identical. Note that  $\mathbb{E}[\mathbb{1}\{\hat{P}_n(a) = 0\}] = \mathbb{P}(\hat{P}_n(a) = 0) = (1 - P(a))^n$ . Therefore, the left hand side (LHS) of the second inequality is

$$\begin{aligned} \text{LHS} &= \sum_{a \in \mathcal{X}} (1 - P(a))^n P(a) \max\{1, -\log P(a)\} \\ &\leq \sum_{a \in \mathcal{X}} \frac{1}{n} \vee \frac{\log n}{n} = \frac{k \log n}{n}, \end{aligned}$$

where we used Lemma 31 and Lemma 32.  $\square$

**Remark 19.** According to [2, Proposition 3], the bound  $k/n$  in (15) is tight up to a constant factor.

Now, we are ready to prove Proposition 16.

*Proof of Proposition 16.* Define  $\Delta_{n,m}(a) := |\psi(P(a), Q(a)) - \psi(\hat{P}_n(a), \hat{Q}_m(a))|$ . We have from the triangle inequality that

$$\Delta_{n,m}(a) \leq \underbrace{|\psi(P(a), Q(a)) - \psi(\hat{P}_n(a), Q(a))|}_{=: \mathcal{T}_1(a)} + \underbrace{|\psi(\hat{P}_n(a), Q(a)) - \psi(\hat{P}_n(a), \hat{Q}_m(a))|}_{=: \mathcal{T}_2(a)}.$$

Since  $\hat{P}_n(a) = 0$  or  $\hat{P}_n(a) \geq 1/n$ , the approximate Lipschitz lemma (Lemma 14) gives

$$\mathcal{T}_1(a) \leq \begin{cases} P(a) (C_1 \max\{1, \log(1/P(a))\} + C_0^* \vee C_2), & \text{if } \hat{P}_n(a) = 0, \\ |P(a) - \hat{P}_n(a)| (C_1 \log n + C_0^* \vee C_2), & \text{else.} \end{cases}$$

Consequently, Lemma 17 yields

$$\begin{aligned} \sum_{a \in \mathcal{X}} \mathbb{E}[\mathcal{T}_1] &\leq \sum_{a \in \mathcal{X}} \mathbb{E} \left[ \mathbb{1}\{\hat{P}_n(a) = 0\} P(a) (C_1 \max\{1, \log(1/P(a))\} + C_0^* \vee C_2) \right] \\ &\quad + \sum_{a \in \mathcal{X}} \mathbb{E} \left[ |\hat{P}_n(a) - P(a)| \right] (C_1 \log n + C_0^* \vee C_2) \\ &\leq (C_1 + C_0^* \vee C_2) \beta_n(P) + (C_1 \log n + C_0^* \vee C_2) \alpha_n(P). \end{aligned}$$

Since  $\psi(p, q) = qf(p/q) = pf^*(q/p)$ , an analogous bound holds for  $\mathcal{T}_2$  with the appropriate adjustment of constants. Hence, the inequality (13) holds. Moreover, when  $k < \infty$ , the inequality (14) follows by invoking again Lemma 18 and Lemma 17.  $\square$

Invoking Proposition 10 and Proposition 16 for the interpolated KL divergence leads to the following result.

**Proposition 20.** Assume that  $k = |\text{Supp}(P)| \vee |\text{Supp}(Q)| < \infty$ . For any  $\lambda \in (0, 1)$ , it holds that

$$\begin{aligned} & \mathbb{E} \left| \text{KL}_\lambda(\hat{P}_n \|\hat{Q}_m) - \text{KL}_\lambda(P \| Q) \right| \\ & \leq \left[ \left( 1 + \frac{(1-\lambda)^2}{\lambda} \right) \log(n \wedge m) + \left( \log \frac{1}{\lambda} - 1 + \lambda \right) \vee \frac{1}{2} + (1-\lambda) \vee \frac{1-\lambda}{8\lambda} \right] \\ & \quad \times \left( \sqrt{\frac{k}{n \wedge m}} + \frac{k}{n \wedge m} \right). \end{aligned}$$

Moreover, for any  $\lambda_{n,m} \in (0, 0.5)$ ,

$$\begin{aligned} & \mathbb{E} \sup_{\lambda \in [\lambda_{n,m}, 1 - \lambda_{n,m}]} \left[ \left| \text{KL}_\lambda(\hat{P}_n \|\hat{Q}_m) - \text{KL}_\lambda(P \| Q) \right| + \left| \text{KL}_{1-\lambda}(\hat{Q}_m \|\hat{P}_n) - \text{KL}_{1-\lambda}(Q \| P) \right| \right] \\ & \leq 2 \left( (1 + 1/\lambda_{n,m}) \log n + \log \frac{1}{\lambda_{n,m}} \vee \frac{1}{2} + 1 \vee \frac{1}{8\lambda_{n,m}} \right) \left( \sqrt{\frac{k}{n \wedge m}} + \frac{k}{n \wedge m} \right). \end{aligned}$$

*Proof.* We only prove the second inequality. The first one is a direct consequence of Proposition 10 and Proposition 16. From the proof of Proposition 16 we have

$$\begin{aligned} & \left| \text{KL}_\lambda(\hat{P}_n \|\hat{Q}_m) - \text{KL}_\lambda(P \| Q) \right| \\ & \leq \sum_{a \in \mathcal{X}} \mathbb{1}\{\hat{P}_n(a) = 0\} P(a) (C_1 \max\{1, \log(1/P(a))\} + C_0^* \vee C_2) \\ & \quad + \sum_{a \in \mathcal{X}} \mathbb{1}\{\hat{Q}_m(a) = 0\} Q(a) (C_1^* \max\{1, \log(1/Q(a))\} + C_0 \vee C_2^*) \\ & \quad + \sum_{a \in \mathcal{X}} |P(a) - \hat{P}_n(a)| (C_1 \log n + C_0^* \vee C_2) + \sum_{a \in \mathcal{X}} |Q(a) - \hat{Q}_m(a)| (C_1^* \log m + C_0 \vee C_2^*). \end{aligned}$$

Note that, for the intepolated KL divergence, we have

$$\begin{aligned} C_0 &= 1 - \lambda \leq 1, \quad C_0^* = \log \frac{1}{\lambda} - 1 + \lambda \leq \log \frac{1}{\lambda_{n,m}} \\ C_1 &= 1, \quad C_1^* = \frac{(1-\lambda)^2}{\lambda} \leq \frac{1}{\lambda_{n,m}} \\ C_2 &= 1/2, \quad C_2^* = \frac{1-\lambda}{8\lambda} \leq \frac{1}{8\lambda_{n,m}} \end{aligned}$$

for all  $\lambda \in [\lambda_{n,m}, 1 - \lambda_{n,m}]$ . The claim then follows from the same steps of Proposition 16.  $\square$

## D.2 Concentration bound

We now state and prove the concentration bound for general  $f$ -divergences which satisfy our regularity assumptions. We start by considering concentration around the expectation.

**Proposition 21.** Consider the  $f$ -divergence  $D_f$  where  $f$  satisfies Assumptions (A1)-(A3). For any  $t > 0$  and any discrete distributions  $P, Q$ , we have,

$$\mathbb{P} \left( |D_f(\hat{P}_n \|\hat{Q}_m) - \mathbb{E}[D_f(\hat{P}_n \|\hat{Q}_m)]| > \varepsilon \right) \leq 2 \exp \left( - \frac{(n \wedge m) \varepsilon^2}{2(c_1 \log(n \wedge m) + c_2)^2} \right),$$

where  $c_1 = C_1 + C_1^*$  and  $c_2 = C_2 \vee C_0^* + C_2^* \vee C_0$ .

*Proof.* We first establish that  $D_f$  satisfies the bounded deviation property and then invoke McDiarmid's inequality.

We start with some notation. As before, define  $\psi(p, q) = qf(p/q)$ . Without loss of generality, let  $\mathcal{X} = \text{Supp}(P) \cup \text{Supp}(Q)$ . Define the function  $\Phi : \mathcal{X}^{n+m} \rightarrow \mathbb{R}$  so that

$$\Phi(X_1, \dots, X_n, Y_1, \dots, Y_m) = D_f(\hat{P}_n \|\hat{Q}_m).$$

We now show the bounded deviation property of  $\Phi$ . Fix some  $T = (x_1, \dots, x_n, y_1, \dots, y_m) \in \mathcal{X}^{n+m}$  and let  $T' = (x'_1, \dots, x'_n, y'_1, \dots, y'_m) \in \mathcal{X}^{n+m}$  be such that  $T$  and  $T'$  differ only on  $x_i = a \neq a' = x'_i$ . Suppose the number of occurrences of  $a$  in the  $x$ -component of  $T$  is  $l$  and of  $a'$  is  $l'$ , while their corresponding  $y$ -components are  $mq$  and  $mq'$  respectively. We now have

$$\begin{aligned} |\Phi(T') - \Phi(T)| &= \left| \psi\left(\frac{s-1}{n}, q\right) - \psi\left(\frac{s}{n}, q\right) + \psi\left(\frac{s'+1}{n}, q'\right) - \psi\left(\frac{s'}{n}, q'\right) \right| \\ &\leq \left| \psi\left(\frac{s-1}{n}, q\right) - \psi\left(\frac{s}{n}, q\right) \right| + \left| \psi\left(\frac{s'+1}{n}, q'\right) - \psi\left(\frac{s'}{n}, q'\right) \right| \\ &\leq \frac{2}{n}(C_1 \log n + C_0^* \vee C_2) =: B_i, \end{aligned}$$

where we used the triangle inequality first and then invoked Lemma 14. Likewise, if  $A$  and  $A'$  differ only in  $y_i$  and  $y'_i$ , an analogous argument gives

$$|\Phi(T') - \Phi(T)| \leq \frac{2}{m}(C_1^* \log m + C_0 \vee C_2^*) =: B_i^*.$$

With this we can use McDiarmid's inequality (cf. Theorem 29) to bound

$$\mathbb{P}\left(|D_f(\hat{P}_n \|\hat{Q}_m) - \mathbb{E}[D_f(\hat{P}_n \|\hat{Q}_m)]| > \varepsilon\right) \leq h(\varepsilon),$$

where

$$h(\varepsilon) = 2 \exp\left(-\frac{2\varepsilon^2}{\sum_{i=1}^n B_i^2 + \sum_{i=n+1}^{n+m} (B_i^*)^2}\right) \leq 2 \exp\left(-\frac{(n \wedge m)\varepsilon^2}{2(c_1 \log(n \wedge m) + c_2)^2}\right).$$

□

Hence, the concentration bound around the population  $f$ -divergence follows directly from Proposition 16 and Proposition 21.

**Theorem 22.** *Assume that  $P$  and  $Q$  are discrete and let  $k = |\text{Supp}(P)| \vee |\text{Supp}(Q)| \in \mathbb{N} \cup \{\infty\}$ . For any  $\delta \in (0, 1)$ , it holds that, with probability at least  $1 - \delta$ ,*

$$\begin{aligned} |D_f(\hat{P}_n \|\hat{Q}_m) - D_f(P\|Q)| &\leq (c_1 \log(n \wedge m) + c_2) \sqrt{\frac{2}{n \wedge m} \log \frac{2}{\delta}} \\ &\quad + (C_1 \log n + C_0^* \vee C_2) \alpha_n(P) + (C_1^* \log m + C_0 \vee C_2^*) \alpha_m(Q) \\ &\quad + (C_1 + C_0^* \vee C_2) \beta_n(P) + (C_1^* + C_0 \vee C_2^*) \beta_m(Q). \end{aligned}$$

Furthermore, if  $k < \infty$ , then, with probability at least  $1 - \delta$ ,

$$|D_f(\hat{P}_n \|\hat{Q}_m) - D_f(P\|Q)| \leq (c_1 \log(n \wedge m) + c_2) \left( \sqrt{\frac{2}{n \wedge m} \log \frac{2}{\delta}} + \sqrt{\frac{k}{n \wedge m}} + \frac{k}{n \wedge m} \right).$$

*Proof of Theorem 22.* We only prove the second inequality. The first one follows from a similar argument. According to Proposition 16, we have

$$\begin{aligned} & \left| D_f(\hat{P}_n \|\hat{Q}_m) - \mathbb{E}[D_f(\hat{P}_n \|\hat{Q}_m)] \right| \\ & \geq \left| D_f(\hat{P}_n \|\hat{Q}_m) - D_f(P\|Q) \right| - \left| \mathbb{E}[D_f(\hat{P}_n \|\hat{Q}_m)] - D_f(P\|Q) \right| \\ & \geq \left| D_f(\hat{P}_n \|\hat{Q}_m) - D_f(P\|Q) \right| - (c_1 \log(n \wedge m) + c_2) \left( \sqrt{\frac{k}{n \wedge m}} + \frac{k}{n \wedge m} \right). \end{aligned}$$

By Proposition 21, it holds that

$$\mathbb{P} \left( \left| D_f(\hat{P}_n \|\hat{Q}_m) - D_f(P\|Q) \right| > \varepsilon + (c_1 \log(n \wedge m) + c_2) \left( \sqrt{\frac{k}{n \wedge m}} + \frac{k}{n \wedge m} \right) \right) \leq h(\varepsilon),$$

where

$$h(\varepsilon) = 2 \exp \left( -\frac{(n \wedge m) \varepsilon^2}{2(c_1 \log(n \wedge m) + c_2)^2} \right).$$

The claim then follows from setting  $h(\varepsilon) = \delta$  and solving for  $\varepsilon$ .  $\square$

## E Add-constant smoothing

In this section, we apply add-constant smoothing to estimate the  $f$ -divergences and study its statistical error.

For notational simplicity, we assume that  $P$  and  $Q$  are supported on a common finite alphabet with size  $k < \infty$ . Without loss of generality, let  $\mathcal{X}$  be the support. Consider  $P \in \mathcal{P}(\mathcal{X})$  and an i.i.d. sample  $\{X_i\}_{i=1}^n \sim P$ . The add-constant estimator of  $P$  is defined by

$$\hat{P}_{n,b}(a) = \frac{N_a + b}{n + kb}, \quad \text{for all } a \in \mathcal{X},$$

where  $b > 0$  is a constant and  $N_a = |\{i \in [n] : X_i = a\}|$  is the number of times the symbol  $a$  appears in the sample. In practice,  $b = b_a$  could be different depending on the value of  $N_a$ , but we use the same constant  $b$  for simplicity. Similarly, We define  $\hat{Q}_{m,b}$  with  $M_a = |\{i \in [m] : Y_i = a\}|$ . The goal is to upper bound the statistical error

$$\mathbb{E} \left| D_f(P\|Q) - D_f(\hat{P}_{n,b} \|\hat{Q}_{m,b}) \right| \tag{17}$$

under Assumption 8.

Compared to the statistical error of the plug-in estimator, a key difference is that each entry in the add-constant estimator is at least  $(n + kb)^{-1} \wedge (m + kb)^{-1}$ . Hence, we can directly apply the approximate Lipschitz lemma without the need to control the missing mass part. Another difference is that the total variation distance is now between the add-constant estimator and its population counterpart, which can be bounded as follows.

**Lemma 23.** *Assume that  $k = \text{Supp}(P) < \infty$ . Then, for any  $b > 0$ ,*

$$\sum_{a \in \mathcal{X}} \mathbb{E} \left| \hat{P}_{n,b}(a) - P(a) \right| \leq \sum_{a \in \mathcal{X}} \frac{\sqrt{n P(a)(1 - P(a))} + b k |P(a) - 1/k|}{n + kb} \leq \frac{\sqrt{kn} + 2b(k-1)}{n + kb}.$$

*Proof.* Note that

$$\left| \hat{P}_{n,b}(a) - P(a) \right| = \left| \frac{N_a - nP(a)}{n + kb} + \frac{b(1 - kP(a))}{n + kb} \right| \leq \left| \frac{N_a - nP(a)}{n + kb} \right| + \left| \frac{b(1 - kP(a))}{n + kb} \right|.$$

Using Jensen's inequality, we have

$$\begin{aligned} \sum_{a \in \mathcal{X}} \mathbb{E} \left| \hat{P}_{n,b}(a) - P(a) \right| &\leq \sum_{a \in \mathcal{X}} \left[ \sqrt{\mathbb{E} \left| \frac{N_a - nP(a)}{n + kb} \right|^2} + \frac{c|1 - kP(a)|}{n + kb} \right] \\ &= \sum_{a \in \mathcal{X}} \left[ \frac{\sqrt{nP(a)(1 - P(a))}}{n + kb} + \frac{bk|1/k - P(a)|}{n + kb} \right]. \end{aligned}$$

We claim that

$$\sum_{a \in \mathcal{X}} \left| P(a) - \frac{1}{k} \right| \leq \frac{2(k-1)}{k}.$$

If this is true, we have

$$\sum_{a \in \mathcal{X}} \mathbb{E} \left| \hat{P}_{n,b}(a) - P(a) \right| \leq \frac{\sqrt{kn} + 2b(k-1)}{n + kb},$$

since  $\sum_{a \in \mathcal{X}} \sqrt{P(a)(1 - P(a))} \leq \sqrt{k}$ . It then remains to prove the claim. Take  $a_1, a_2 \in \mathcal{X}$  such that  $P(a_1) \geq k^{-1} \geq P(a_2)$ . It is clear that

$$\begin{aligned} \left| P(a_1) - \frac{1}{k} \right| + \left| P(a_2) - \frac{1}{k} \right| &\leq \left| P(a_1) + P(a_2) - \frac{1}{k} \right| + \left| P(a_2) - P(a_1) - \frac{1}{k} \right| \\ &= P(a_1) + P(a_2). \end{aligned}$$

Repeating this argument gives

$$\sum_{a \in \mathcal{X}} \left| P(a) - \frac{1}{k} \right| \leq 1 - \frac{1}{k} + \frac{k-1}{k} = \frac{2(k-1)}{k}.$$

□

The next proposition gives the upper bound for the statistical error of the add-constant estimator.

**Proposition 24.** *Suppose that  $f$  satisfies Assumption 8 and  $k = |\mathcal{X}| < \infty$ . We have, for any  $n, m \geq 3$ ,*

$$\begin{aligned} \mathbb{E} |D_f(P\|Q) - D_f(\hat{P}_{n,b}\|\hat{Q}_{m,b})| &\leq \left[ \frac{n\alpha_n(P)}{n + kb} + \gamma_{n,k}(P) \right] (C_1 \log(n/b + k) + C_0^* \vee C_2) \\ &\quad + \left[ \frac{m\alpha_m(Q)}{m + kb} + \gamma_{m,k}(Q) \right] (C_1^* \log(m/b + k) + C_0 \vee C_2^*) \\ &\leq (C_1 \log(n/b + k) + C_0^* \vee C_2) \frac{\sqrt{kn} + 2b(k-1)}{n + kb} \\ &\quad + (C_1^* \log(m/b + k) + C_0 \vee C_2^*) \frac{\sqrt{km} + 2b(k-1)}{m + kb}, \end{aligned}$$

where  $\gamma_{n,k}(P) = (n + bk)^{-1}bk \sum_{a \in \mathcal{X}} |P(a) - 1/k|$ .

*Proof.* Following the proof of Proposition 16, we define

$$\Delta_{n,m}(a) := \left| \psi(P(a), Q(a)) - \psi(\hat{P}_{n,b}(a), \hat{Q}_{m,b}(a)) \right|.$$

We have from the triangle inequality that

$$\Delta_{n,m}(a) \leq \underbrace{\left| \psi(P(a), Q(a)) - \psi(\hat{P}_{n,b}(a), Q(a)) \right|}_{=: \mathcal{T}_1(a)} + \underbrace{\left| \psi(\hat{P}_{n,b}(a), Q(a)) - \psi(\hat{P}_{n,b}(a), \hat{Q}_{m,b}(a)) \right|}_{=: \mathcal{T}_2(a)}.$$

Since  $\hat{P}_{n,b}(a) \geq b/(n+kb)$ , the approximate Lipschitz lemma (Lemma 14) gives

$$\mathcal{T}_1(a) \leq |P(a) - \hat{P}_{n,b}(a)| (C_1 \log(n/b+k) + C_0^* \vee C_2),$$

By lemma 23, it holds that

$$\begin{aligned} \frac{\sum_{a \in \mathcal{X}} \mathbb{E}[\mathcal{T}_1(a)]}{C_1 \log(n/b+k) + C_0^* \vee C_2} &\leq \sum_{a \in \mathcal{X}} \left[ \frac{\sqrt{n}P(a)}{n+kb} + \frac{bk|1/k - P(a)|}{n+kb} \right] = \frac{n\alpha_n(P)}{n+kb} + \gamma_{n,k}(P) \\ &\leq \frac{\sqrt{kn} + 2b(k-1)}{n+kb}. \end{aligned}$$

Since  $\psi(p, q) = qf(p/q) = pf^*(q/p)$ , an analogous bound holds for  $\mathcal{T}_2(a)$  with the appropriate adjustment of constants and the sample size. Putting these together, we get,

$$\begin{aligned} \mathbb{E}|D_f(P\|Q) - D_f(\hat{P}_{n,b}\|\hat{Q}_{m,b})| &\leq \mathbb{E} \left[ \sum_{a \in \mathcal{X}} |\Delta_n(a)| \right] \\ &\leq \left[ \frac{n\alpha_n(P)}{n+kb} + \gamma_{n,k}(P) \right] (C_1 \log(n/b+k) + C_0^* \vee C_2) \\ &\quad + \left[ \frac{m\alpha_m(Q)}{m+kb} + \gamma_{m,k}(Q) \right] (C_1^* \log(m/b+k) + C_0 \vee C_2^*) \\ &\leq (C_1 \log(n/b+k) + C_0^* \vee C_2) \frac{\sqrt{kn} + 2b(k-1)}{n+kb} \\ &\quad + (C_1^* \log(m/b+k) + C_0 \vee C_2^*) \frac{\sqrt{km} + 2b(k-1)}{m+kb}. \end{aligned}$$

□

The concentration bound for the add-constant estimator can be proved similarly.

## F Quantization error

In this section, we study the quantization error of  $f$ -divergences, i.e.,

$$\inf_{|\mathcal{S}| \leq k} |D_f(P\|Q) - D_f(P_{\mathcal{S}}\|Q_{\mathcal{S}})|, \quad (18)$$

where the infimum is over all partitions of  $\mathcal{X}$  of size no larger than  $k$ , and  $P_{\mathcal{S}}$  and  $Q_{\mathcal{S}}$  are the quantized versions of  $P$  and  $Q$  according to  $\mathcal{S}$ , respectively. Note that we do not assume  $\mathcal{X}$  to be discrete in this section.

Our analysis is inspired by the following result, which shows that the  $f$ -divergence can be approximated by its quantized counterpart; see, e.g., [17, Theorem 6].

**Theorem 25.** *For any  $P, Q \in \mathcal{P}(\mathcal{X})$ , it holds that*

$$D_f(P\|Q) = \sup_{\mathcal{S}} D_f(P_{\mathcal{S}}\|Q_{\mathcal{S}}), \quad (19)$$

where the supremum is over all finite partitions of  $\mathcal{X}$ .

The next theorem holds for general  $f$ -divergences without the requirement of Assumption 8.

**Theorem 26.** *For any  $k \geq 1$ , we have*

$$\sup_{P,Q} \inf_{|\mathcal{S}| \leq 2k} |D_f(P\|Q) - D_f(P_{\mathcal{S}}\|Q_{\mathcal{S}})| \leq \frac{f(0) + f^*(0)}{k}.$$

*Proof.* Assume  $f(0) + f^*(0) < \infty$ . Otherwise, there is nothing to prove. Fix two distributions  $P, Q$  over  $\mathcal{X}$ . Partition the measurable space  $\mathcal{X}$  into

$$\mathcal{X}_1 = \left\{ x \in \mathcal{X} : \frac{dP}{dQ}(x) \leq 1 \right\}, \quad \text{and,} \quad \mathcal{X}_2 = \left\{ x \in \mathcal{X} : \frac{dP}{dQ}(x) > 1 \right\},$$

so that

$$D_f(P\|Q) = \int_{\mathcal{X}_1} f\left(\frac{dP}{dQ}(x)\right) dQ(x) + \int_{\mathcal{X}_2} f^*\left(\frac{dQ}{dP}(x)\right) dP(x) =: D_f^+(P\|Q) + D_{f^*}^+(Q\|P).$$

We quantize  $\mathcal{X}_1$  and  $\mathcal{X}_2$  separately, starting with  $\mathcal{X}_1$ . Define sets  $S_1, \dots, S_k$  as

$$S_m = \left\{ x \in \mathcal{X}_1 : \frac{f(0)(m-1)}{k} \leq f\left(\frac{dP}{dQ}(x)\right) < \frac{f(0)m}{k} \right\},$$

where the last set  $S_k$  is also extended to include  $\{x \in \mathcal{X}_1 : f((dP/dQ)(x)) = f(0)\}$ . Since  $f$  is nonincreasing on  $(0, 1]$ , it follows that  $\sup_{x \in \mathcal{X}_1} f((dP/dQ)(x)) \leq f(0)$ . As a result, the collection  $\mathcal{S} = \{S_1, \dots, S_k\}$  is a partition of  $\mathcal{X}_1$ . This gives

$$\frac{f(0)}{k} \sum_{m=1}^k (m-1) Q[S_m] \leq D_f^+(P\|Q) \leq \frac{f(0)}{k} \sum_{m=1}^k m Q[S_m]. \quad (20)$$

Further, since  $f$  is nonincreasing on  $(0, 1]$ , we also have

$$\frac{f(0)(m-1)}{k} \leq f\left(\sup_{x \in F_m} \frac{dP}{dQ}(x)\right) \leq f\left(\frac{P[F_m]}{Q[F_m]}\right) \leq f\left(\inf_{x \in F_m} \frac{dP}{dQ}(x)\right) \leq \frac{f(0)m}{k}.$$

Hence, it follows that

$$\frac{f(0)}{k} \sum_{m=1}^k (m-1) Q[S_m] \leq D_f^+(P_{\mathcal{S}_1}\|Q_{\mathcal{S}_1}) \leq \frac{f(0)}{k} \sum_{m=1}^k m Q[S_m]. \quad (21)$$

Putting (20) and (21) together gives

$$\inf_{|\mathcal{S}_1| \leq k} |D_f^+(P\|Q) - D_f^+(P_{\mathcal{S}_1}\|Q_{\mathcal{S}_1})| \leq \frac{f(0)}{k} \sum_{m=1}^k Q[S_m] \leq \frac{f(0)}{k}, \quad (22)$$

since  $\sum_{m=1}^k Q[S_m] = Q[\mathcal{X}_1] \leq 1$ . Repeating the same argument with  $P$  and  $Q$  interchanged and replacing  $f$  by  $f^*$  gives

$$\inf_{|\mathcal{S}_2| \leq k} |D_{f^*}^+(Q\|P) - D_{f^*}^+(Q_{\mathcal{S}_2}\|P_{\mathcal{S}_2})| \leq \frac{f^*(0)}{k}. \quad (23)$$

To complete the proof, we upper bound the inf of  $\mathcal{S}$  over all partitions of  $\mathcal{X}$  with  $|\mathcal{S}| = k$  by the inf over  $\mathcal{S} = \mathcal{S}_1 \cup \mathcal{S}_2$  with partitions  $\mathcal{S}_1$  of  $\mathcal{X}_1$  and  $\mathcal{S}_2$  of  $\mathcal{X}_2$ , and  $|\mathcal{S}_1| = |\mathcal{S}_2| = k$ . Now, under this partitioning, we have,

$D_f^+(P_S\|Q_S) = D_f^+(P_{S_1}\|Q_{S_1})$  and  $D_{f^*}^+(Q_S\|P_S) = D_{f^*}^+(Q_{S_2}\|P_{S_2})$ . Putting this together with the triangle inequality, we get,

$$\begin{aligned}
& \inf_{|\mathcal{S}| \leq 2k} \left| D_f(P\|Q) - D_f(P_S\|Q_S) \right| \\
& \leq \inf_{\mathcal{S}=\mathcal{S}_1 \cup \mathcal{S}_2} \left\{ \left| D_f^+(P\|Q) - D_f^+(P_S\|Q_S) \right| + \left| D_{f^*}^+(Q\|P) - D_{f^*}^+(Q_{S_2}\|P_{S_2}) \right| \right\} \\
& = \inf_{|\mathcal{S}_1| \leq k} \left| D_f^+(P\|Q) - D_f^+(P_{S_1}\|Q_{S_1}) \right| + \inf_{|\mathcal{S}_2| \leq k} \left| D_{f^*}^+(Q\|P) - D_{f^*}^+(Q_{S_2}\|P_{S_2}) \right| \\
& \leq \frac{f(0) + f^*(0)}{k}.
\end{aligned}$$

□

Now, combining Proposition 16 and Theorem 26 leads to an upper bound for the overall estimation error.

**Theorem 27.** *Let  $\mathcal{S}_k$  be a partition of  $\mathcal{X}$  such that  $|\mathcal{S}| = k \geq 2$  and its quantization error satisfies the bound in Theorem 26, i.e.,*

$$|D_f(P\|Q) - D_f(P_{\mathcal{S}_k}\|Q_{\mathcal{S}_k})| \leq \frac{f(0) + f^*(0)}{k}.$$

Then, for any  $n, m \geq 3$ ,

$$\begin{aligned}
& \mathbb{E} \left| D_f(\hat{P}_{\mathcal{S}_k, n}\|\hat{Q}_{\mathcal{S}_k, m}) - D_f(P\|Q) \right| \\
& \leq (C_1 \log n + C_0^* \vee C_2) \alpha_n(P) + (C_1^* \log m + C_0 \vee C_2^*) \alpha_m(Q) \\
& \quad + (C_1 + C_0^* \vee C_2) \beta_n(P) + (C_1^* + C_0 \vee C_2^*) \beta_m(Q) + \frac{f(0) + f^*(0)}{k} \\
& \leq (c_1 \log(n \wedge m) + c_2) \left( \sqrt{\frac{k}{n \wedge m}} + \frac{k}{n \wedge m} \right) + \frac{f(0) + f^*(0)}{k},
\end{aligned}$$

where  $c_1 = C_1 + C_1^*$  and  $c_2 = C_2 \vee C_0^* + C_2^* \vee C_0$ .

According to Theorem 27, a good choice of quantization level  $k$  is of order  $\Theta(n^{-1/3})$  which balances between the two types of errors.

## G Experimental details

We investigate the empirical behavior of the frontier integral on both synthetic and real data. Our main findings are: 1) the statistical error bound is tight—it approximately reveals the rate of convergence of the plug-in estimator. 2) The smoothed distribution estimators improve the estimation accuracy. For simplicity, we consider  $m = n$  throughout this section.

### G.1 Synthetic data

We focus on the case when the support is finite and illustrate the statistical behavior of the frontier integral on synthetic data.

**Settings.** Let  $k = |\mathcal{X}|$  be the support size. Following the experimental settings in [39], we consider three types of distributions: 1) the Zipf( $r$ ) distribution with  $r \in \{0, 1, 2\}$  where  $P(i) \propto i^{-r}$ . Note that Zipf( $r$ ) is regularly varying with index  $-r$ ; see, e.g., [48, Appendix B]. 2) the Step distribution where  $P(i) = 1/2$  for the first half bins and  $P(i) = 3/2$  for the second half bins. 3) the Dirichlet distribution  $\text{Dir}(\alpha)$  with

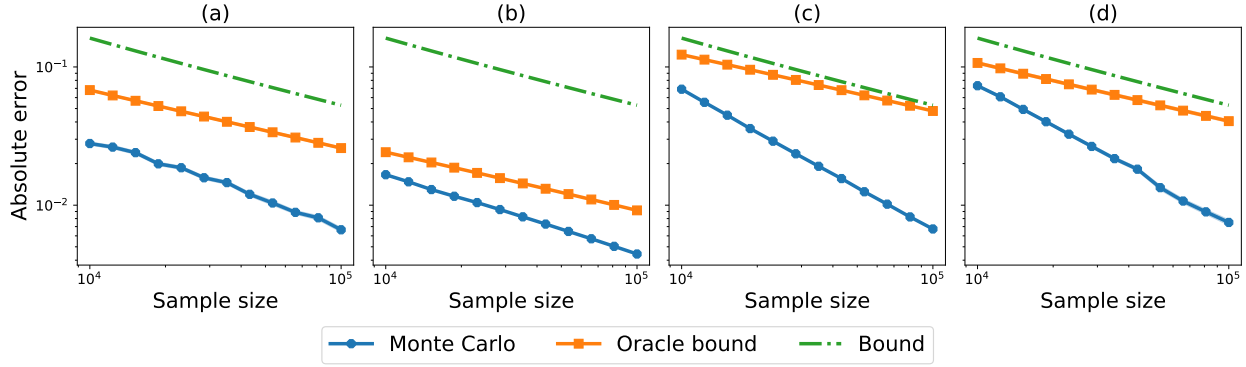


Figure 8: Absolute error versus sample size for the statistical error bounds (4) and the Monte Carlo estimate with  $k = 10^3$  (log-log scale). (a): Zipf(2) and Dir(1); (b): Zipf(2) and Zipf(2); (c): Zipf(0) and Zipf(0); (d): Dir(1) and Dir(1/2). The bounds are scaled by 50.

$\alpha \in \{1/2, 1\}$ . In total, there are 6 different distributions. Since the frontier integral is symmetric, there are 21 different pairs of  $(P, Q)$ . For each pair  $(P, Q)$ , we generate i.i.d. samples of size  $n$  from each of them, and then compute the absolute error  $|\text{FI}(\hat{P}_n, \hat{Q}_n) - \text{FI}(P, Q)|$ . We repeat the process 100 times and report its mean and standard error, which is referred to as the Monte Carlo estimate of the expected absolute error.

**Statistical error.** To study the tightness of the statistical error bounds (4), we compare both the distribution-free bound (“Bound”) and the distribution-dependent bound (“Oracle bound”) with the Monte Carlo estimate (“Monte Carlo”). We call the distribution-free bound the “bound” and the distribution-dependent bound the “oracle bound”. We consider three different experiments. First, we fix the support size  $k = 10^3$  and increase the sample size  $n$  from  $10^3$  to  $10^4$ . Second, we fix  $n = 2 \times 10^4$  and increase  $k$  from 10 to  $10^4$ . Third, we fix  $k = 10^3$  and  $n = 10^4$ , and set  $Q$  to be the Zipf( $r$ ) with  $r$  ranging from 0 to 2. For each of these experiments, we give four typical plots among all pairs of distributions we consider. Note that the two bounds are divided by the same constant for the sake of comparison.

As shown in Figure 8, the two bounds decrease with  $n$  at a similar rate. The oracle bound demonstrates the largest improvement compared to the bound when both  $P$  and  $Q$  have fast-decaying tails (i.e., with index  $-2$ ). In some cases, the Monte Carlo estimate demonstrates a similar rate of convergence as the bounds; while, in other cases, the Monte Carlo estimate can have a faster rate. This suggests that the bound (4) is at least close to being tight up to a multiplicative constant.

Figure 9 shows that the oracle bound increases with  $k$  at a slower rate than the one of the bound. In fact, it is much slower when both  $P$  and  $Q$  decay fast. For the Monte Carlo estimate, it can have either a slower or faster rate than the bound depending on the underlying distributions.

The results for the third experiment is in Figure 10. While the bound remains the same for different tails of  $Q$ , the oracle bound is adapted to the decaying index of  $Q$ . The absolute error of the Monte Carlo estimate is usually increasing in the beginning and then decreasing after some threshold.

**Distribution estimators.** We then compare 4 different distribution estimators with the empirical measures (“Empirical”) as discussed in [39]. For each  $a \in \mathcal{X}$ , let  $n_a$  be the number of times  $a$  appears in the sample  $\{X_i\}_{i=1}^n$  and let  $\varphi_t$  be the number of symbols appearing  $t$  times in the sample. The (*modified*) *Good-Turing* estimator is defined as  $\hat{P}_{\text{GT},n}(a) \propto n_a$  if  $n_a > \varphi_{n_a+1}$  and  $\hat{P}_{\text{GT},n}(a) \propto [\varphi_{n_a+1} + 1](n_a + 1)/\varphi_{n_a}$  otherwise. The remaining three estimators are all based on the add- $b$  smoothing introduced in Section 3. For the *Laplace* estimator, the parameter  $b \equiv 1$ . For the *Krichevsky-Trofimov* estimator, the parameter  $b \equiv 1/2$ . For the *Braess-Sauer* estimator, the parameter  $b = b_a$  is data-dependent and chosen as  $b_a = 1/2$  if  $n_a = 0$ ,  $b_a = 1$  if  $n_a = 1$  and  $b_a = 3/4$  otherwise.

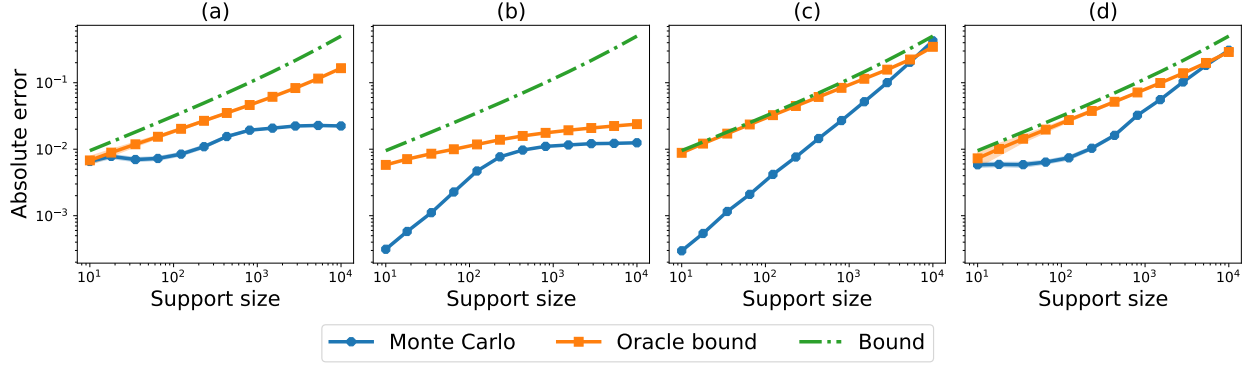


Figure 9: Absolute error versus support size for the statistical error bounds (4) and the Monte Carlo estimate with  $n = 2 \times 10^4$  (log-log scale). (a): Zipf(2) and  $\text{Dir}(1)$ ; (b): Zipf(2) and Zipf(2); (c): Zipf(0) and Zipf(0); (d):  $\text{Dir}(1)$  and  $\text{Dir}(1/2)$ . The bounds are scaled by 50.

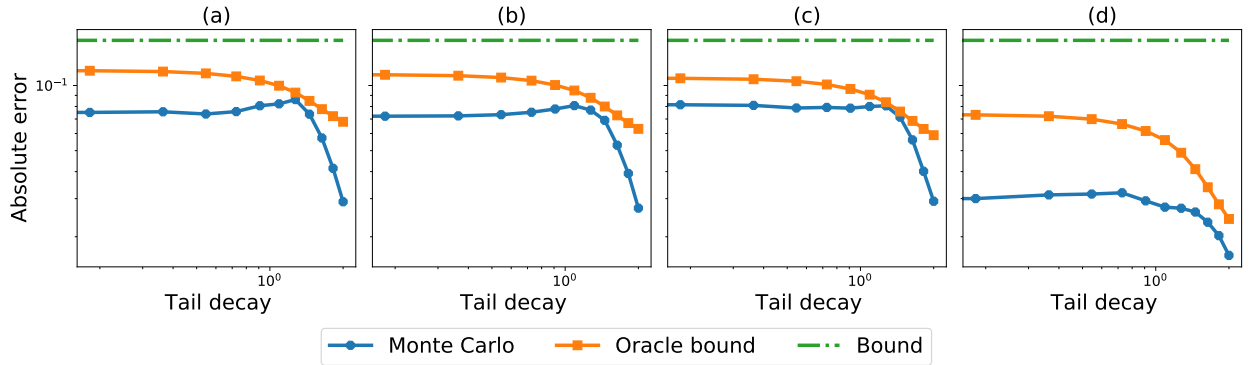


Figure 10: Absolute error versus decaying index of  $Q$  for the statistical error bounds (4) and the Monte Carlo estimate with  $k = 10^3$  and  $n = 10^4$  (log-log scale). (a):  $P \sim \text{Dir}(1)$ ; (b):  $P \sim \text{Dir}(1/2)$ ; (c):  $P \sim \text{Zipf}(1)$ ; (d):  $P \sim \text{Zipf}(2)$ . The bounds are scaled by 50.

We consider the same three experiments as for the statistical error. As shown in Figure 11, the rate of convergence in  $n$  of all estimators are similar except for some fluctuations of the Good-Turing estimator. When  $P = Q$  (i.e., Zipf(1)), the add-constant estimators outperforms the empirical measures slightly while the Good-Turing estimator performs better than the empirical measures for relatively small sample size and performs worse as the sample size increases. When one of the distribution has a fast-decaying tail (i.e.,  $P \sim \text{Zipf}(2)$ ), the absolute error of the add-constant estimators are much larger than the one of empirical measures, while the Good-Turing estimator has a similar performance as empirical measures. When  $P$  and  $Q$  are different and do not have fast-decaying tails, the Krichevsky-Trofimov estimator enjoys the largest improvement compared to the empirical measures.

Figure 12 presents the results for increasing support size. The findings are similar to the ones in the first experiment except that the absolute error is increasing here rather than decreasing.

Figure 13 shows that the Good-Turing estimator is relatively more robust to the tail decaying index than other estimators. When  $P \sim \text{Zipf}(2)$ , the absolute error of the add-constant estimators is much larger than the one of the empirical measures in the beginning and then becomes slightly smaller in the end. In other cases, this behavior is reversed.

To summarize, when two distributions are the same, all estimators performs similarly with the Good-Turing estimator being the worst. When there is one distribution whose tail decays fast, the Good-Turing estimator

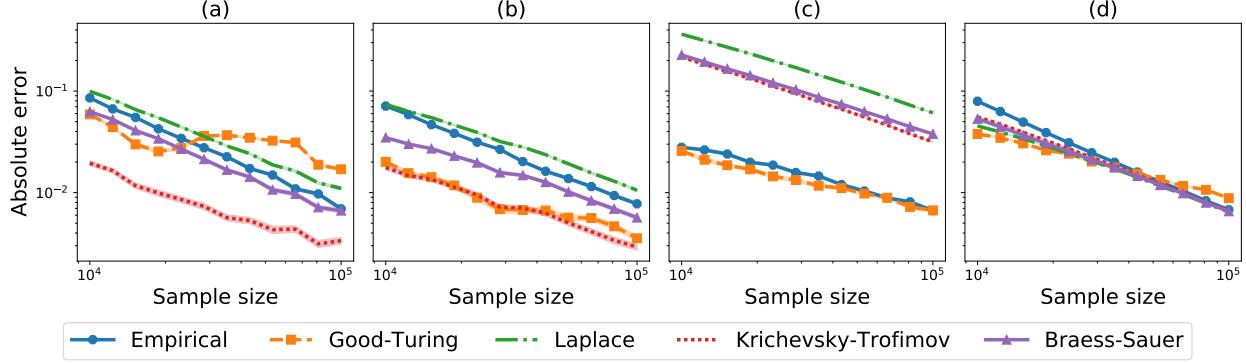


Figure 11: Absolute error versus sample size for different distribution estimators with  $k = 10^3$  (log-log scale). (a): Zipf(1) and Step; (b): Zipf(0) and Dir(1/2); (c): Zipf(2) and Dir(1); (d): Zipf(1) and Zipf(1).

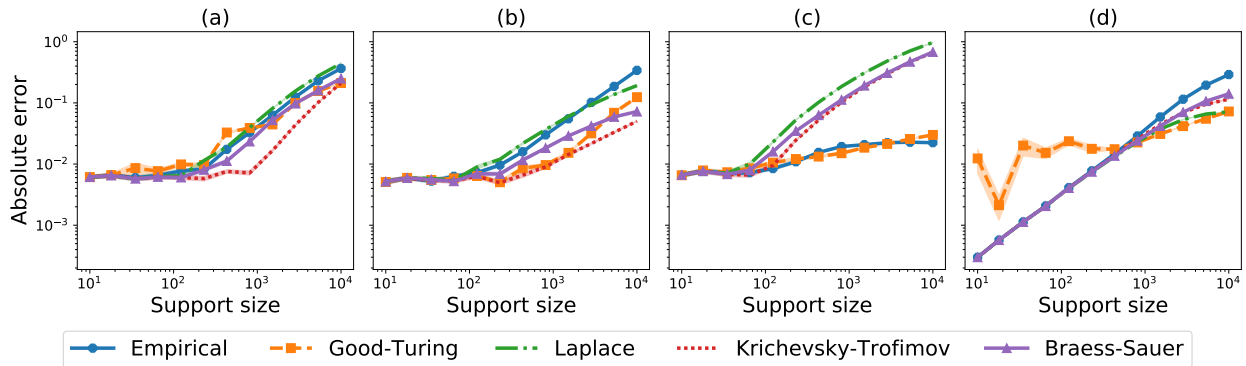


Figure 12: Absolute error versus support size for different distribution estimators with  $n = 2 \times 10^4$  (log-log scale). (a): Zipf(1) and Step; (b): Zipf(0) and Dir(1/2); (c): Zipf(2) and Dir(1); (d): Zipf(1) and Zipf(1).

slightly outperforms the empirical measure; while the add-constant estimators have much larger absolute errors. When the tails of both distributions decay slowly, the Krichevsky-Trofimov estimator has the best performance over all estimators.

**Quantization error.** We study the bound on the quantization error as in (6). Since the absolute error is always zero when  $P = Q$ , we have  $21 - 6 = 15$  different pairs of  $(P, Q)$ . We consider three different quantization strategies: 1) the *uniform* quantization which quantizes the distributions into equally spaced bins based on their original ordering; 2) the *greedy* quantization which sorts the bins according to the ratios  $\{P(a)/Q(a)\}_{a \in \mathcal{X}}$  and then add split one bin at a time so that the frontier integral is maximized; 3) the *oracle* quantization we used to prove (6); see also Figure 14.

As shown in Figure 14, the absolute error of the oracle quantization can have a faster rate than  $O(k^{-1})$  in some cases. To be more specific, when both  $P$  and  $Q$  have slow-decaying tails, its absolute error decays roughly as  $O(k^{-1.7})$ ; when one of them has fast-decaying tail, its absolute error decays slower than  $O(k^{-1})$  in the beginning and then faster than  $O(k^{-1})$ . Comparing different quantization strategies, the oracle quantization always outperforms the greedy one. When either  $P$  or  $Q$  is not ordered, the uniform quantization has the worst performance. When both  $P$  and  $Q$  are ordered, its absolute error is not monotonic—it is quite small in the beginning and then becomes larger.

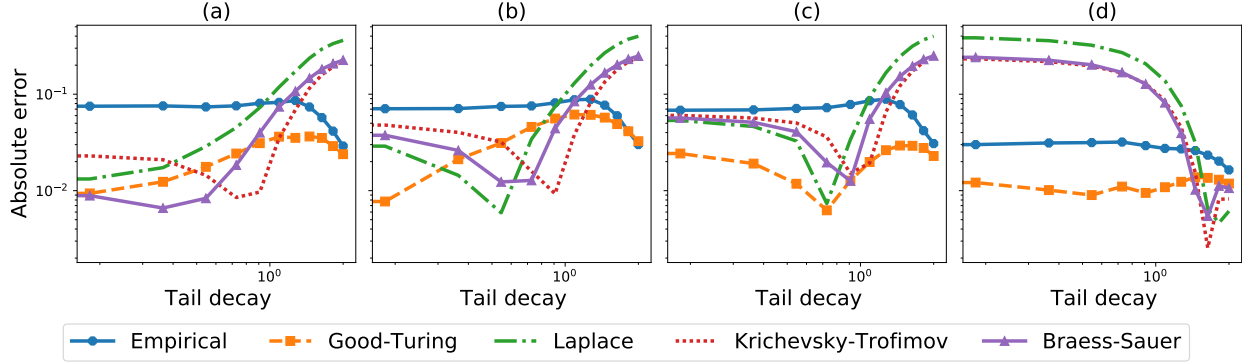


Figure 13: Absolute error versus sample size for different distribution estimators with  $k = 10^3$  and  $n = 10^4$  (log-log scale). (a):  $P \sim \text{Dir}(\mathbf{1})$ ; (b):  $P \sim \text{Step}$ ; (c):  $\text{Zipf}(0)$ ; (d):  $\text{Zipf}(2)$ .

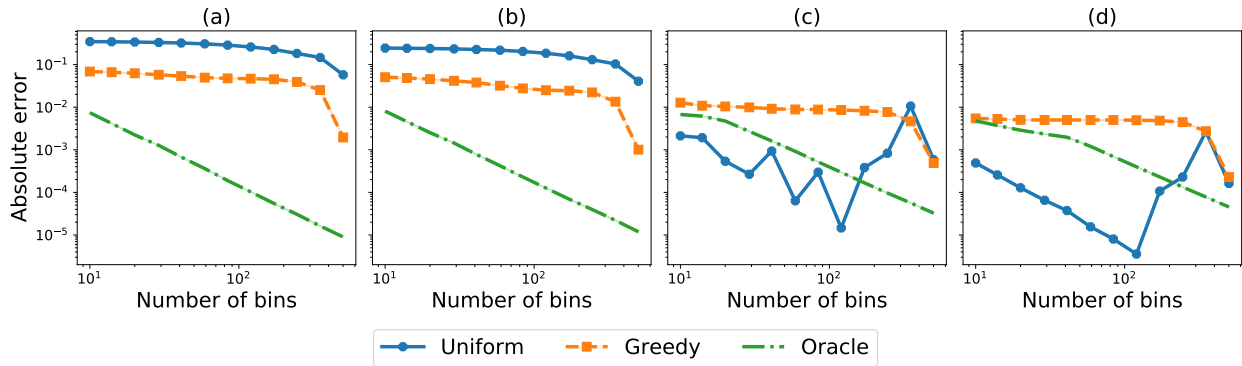


Figure 14: Absolute error versus number of bins for different quantization strategies with support size 600 (log-log scale). (a):  $\text{Dir}(\mathbf{1})$  and  $\text{Dir}(\mathbf{1}/2)$ ; (b):  $\text{Zipf}(0)$  and  $\text{Dir}(\mathbf{1}/2)$ ; (c):  $\text{Zipf}(2)$  and  $\text{Step}$ ; (d):  $\text{Zipf}(1)$  and  $\text{Zipf}(2)$ .

## G.2 Real data

We analyze the performance of the bounds as well as the various smoothed estimators in the context evaluating generative models for images and text using divergence curves. All experiments models are trained on a workstation with 8 Nvidia Quadro RTX GPUs (24G memory each). The image experiments were trained with 2 GPUs at once while the text ones used all 8.

**Tasks and datasets.** We consider two domains: images and text. For the image domain, we train a generative model for the CIFAR-10 dataset [29] based on StyleGAN2-Ada [25]. We use the publicly available code<sup>3</sup> with their default hyperparameters and train on 2 GPUs. In order to enable the code to run faster, we make two architectural simplifications: (a) we reduce the channel dimensions for each convolution layer in the generator from 512 to 256, and, (b) we reduce the number of styled convolution layers for each resolution from 2 to 1. In particular, the latter effectively cuts the number of convolution layers in half. This leads to a 6.6x reduction in running time at the cost of a slightly worse FID [22] of 4.7 rather than the 2.4 of the original network. In order to compute the divergence frontier, we use the test set of 10000 images as the target distribution  $P$  and we sample 10000 images from the generative model as the model distribution  $Q$ .

For the text domain, we finetune a pretrained GPT-2 [41] model with 124M parameters (i.e., GPT-2

<sup>3</sup><https://github.com/NVlabs/stylegan2-ada-pytorch>

small) on the WikiText-103 dataset [35]. We use the open-source HuggingFace Transformers library [57] for training. To form a sufficiently large evaluation set, we finetune on 90% of the wikitext-103 training dataset, and use the remaining 10% plus the validation set as an evaluation set. Finetuning is done on 4 GPUs for 2k iterations, with sequences of 1024 tokens and a batch size of 8 sequences. For generation, we split the evaluation set into 10k sequences of 500 tokens, and split each sequence into a prefix of length 100 and a continuation of length 400. The prefix paired with the continuation (a “completion”) is considered a sample from  $P$ . Using the finetuned model we generate a continuation for each prefix using top- $p$  sampling with  $p = 0.9$ . Each prefix paired with its generated continuation is considered a sample from  $Q$ .

**Settings.** In order to compute the divergence frontier, we jointly quantize  $P$  and  $Q$ , not directly in a raw image/text space, but in a feature space [46, 30, 22]. Specifically, we represent each image by its features from a pretrained ResNet-50 model [20], and each text generation by its terminal hidden state under a pretrained the 774M GPT-2 model (i.e., GPT-2 large). In order to quantize these features, we learn a 4 or 5 dimensional embedding of the image/text features using a deep network which maintains the neighborhood structure of the data while encouraging the features to be uniformly distributed on the unit sphere [45], and simply quantize these embeddings on a uniform lattice with  $k$  bins. For each support size  $k$ , this gives us quantized distributions  $P_{\mathcal{S}_k}, Q_{\mathcal{S}_k}$ . We then sample  $n$  i.i.d points each from these distributions and consider the empirical distributions  $\hat{P}_{\mathcal{S}_k, n}, \hat{Q}_{\mathcal{S}_k, n}$  as well as the add-constant and Good-Turing estimators computed from these samples. We repeat this 100 times to a Monte Carlo estimate of the expected absolute error  $\mathbb{E}|\text{FI}(\hat{P}_{\mathcal{S}_k, n}, \hat{Q}_{\mathcal{S}_k, n}) - \text{FI}(P_{\mathcal{S}_k}, Q_{\mathcal{S}_k})|$  as well as its standard error.

**Statistical error.** We compare the distribution-dependent bound (“oracle bound”) and the distribution-free bound (“bound”) to the Monte Carlo estimates described above. We consider two experiments. First, we fix the support size  $k$  and vary the sample size  $n$  from 100 to 25000. Second, we fix the sample size  $n$  and vary the support size  $k$  from 8 to 2048 in powers of 2.

We observe Figure 15 that both the distribution-free and distribution-dependent bounds decrease with the sample size  $n$  at a similar rate. For  $k = 1024$  or  $k = 2048$ , we observe that the bound has approximately the same slope as the Monte Carlo estimate in log-log scale; this means that they exhibit a near-identical rate in  $n$ . On the other hand, the Monte Carlo estimates exhibit fast rates of convergence than the bound for  $k = 64$  or  $k = 128$ . Therefore, the bounds capture the worst-case behavior of real image and text data.

Next, we see from Figure 16 that the two bounds again exhibit near-identical rates with the support size  $k$ . We observe again that the slope of the Monte Carlo estimate and that of the bounds are close for  $n = 1000$ , indicating a similar scaling with respect to  $k$ . However, the Monte Carlo estimate grows faster than the bound for  $n = 10000$ .

**Distribution estimators.** As in the previous section, we compare the empirical estimator, the (modified) Good-Turing estimator, and three add- $b$  smoothing estimators, namely Laplace, Krichevsky-Trofimov and Braess-Sauer. We consider the same two experiments as for the statistical error.

From Figure 17, we see that for  $n > k$ , we observe similar rates (i.e., similar slopes) for all estimators with respect to the sample size  $n$ . The absolute error of the Good-Turing estimator is the worst among all estimators considered for  $k = 64$  or  $k = 128$  and  $n$  large. However, for  $k = 1024$  or  $k = 2048$ , the empirical estimator is the worst. The various add- $b$  estimators work the best in the regime of  $n < k$ , where each add- $b$  estimator attains the smallest error at a different  $n$ . In particular, the Laplace estimator is the best or close to the best in all each of the settings considered.

Figure 18 shows the corresponding results for varying  $k$ . The results are similar to the previous setting, expect the error increases with  $k$  rather than decreases.

**Performance across training.** Next, we visualize the divergence frontiers and the corresponding frontier integral across training in Figure 19. On the left, we plot the divergence curve at initialization (or with the pretrained model in case of text), at the first checkpoint (“Partly”) and the fully trained model (“Final”). We observe that the divergence frontiers for the fully trained model are closer to the origin than the partially

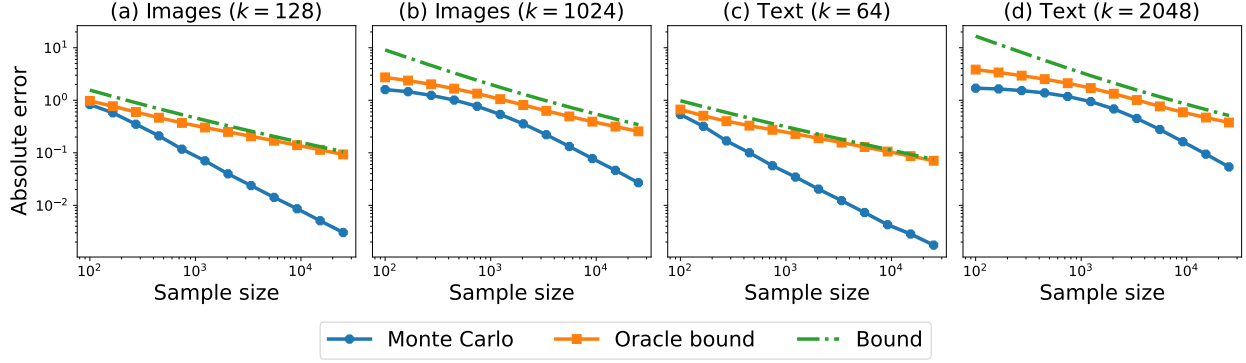


Figure 15: Absolute error versus sample size  $n$  for the statistical error bounds (4) and the Monte Carlo estimate (log-log scale). **Left Two:** Image data (CIFAR-10) with support sizes  $k = 128$  and  $k = 1024$ . **Right Two:** Text data (WikiText-103) with support sizes  $k = 64$  and  $k = 2048$ . The bounds are scaled by 15.

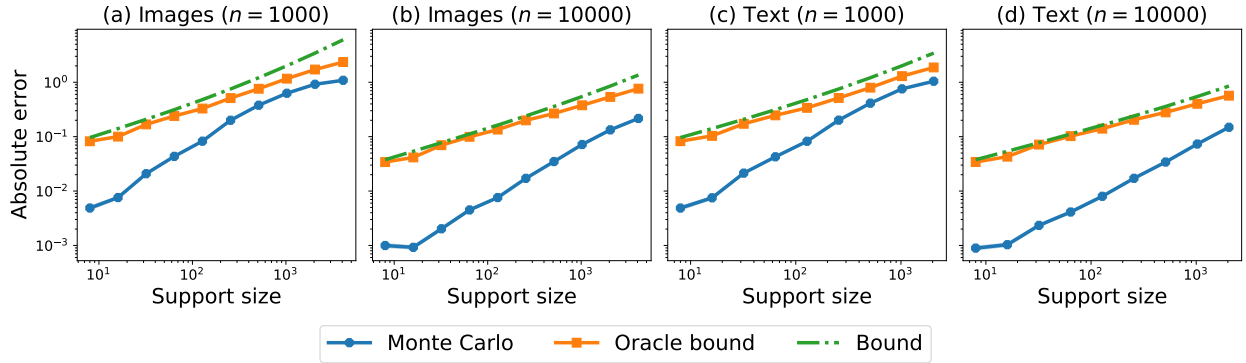


Figure 16: Absolute error versus support size  $k$  for the statistical error bounds (4) and the Monte Carlo estimate (log-log scale). **Left Two:** Image data (CIFAR-10) with sample sizes  $n = 1000$  and  $n = 10000$ . **Right Two:** Text data (WikiText-103) with sample sizes  $n = 1000$  and  $n = 10000$ . The bounds are scaled by 15.

trained ones or the model at initialization. This denotes a smaller loss of precision and recall for the fully trained model. The frontier integral, as a summary statistic, shows the same trend (right).

## H Length of the divergence frontier

In this section, we discuss how the length of the divergence frontier is different from the frontier integral. In particular, we show that the length of the divergence frontier is lower bounded by the Jeffery divergence, which could be unbounded, whereas the frontier integral is always bounded between 0 and 1.

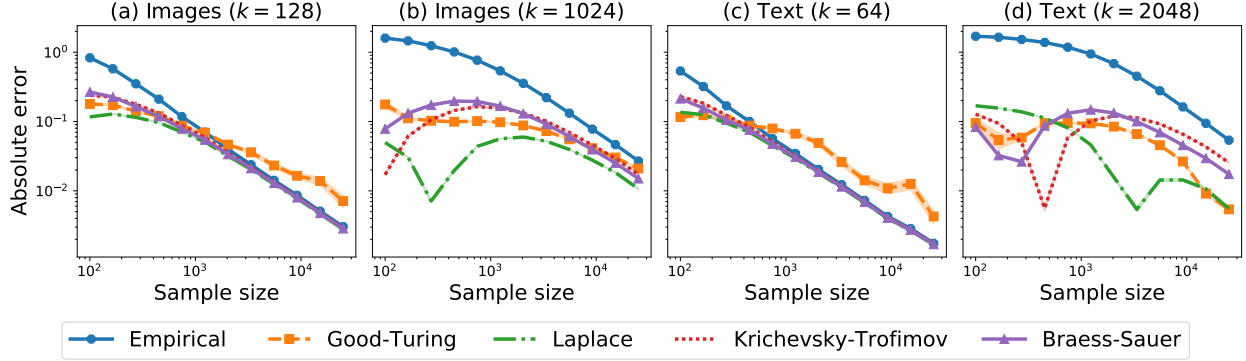


Figure 17: Absolute error versus sample size  $n$  for different distribution estimators. **Left Two:** Image data (CIFAR-10) with support size  $k = 128$  and  $k = 1024$  **Right Two:** Text data (WikiText-103) with support size  $k = 64$  and  $k = 2048$ .

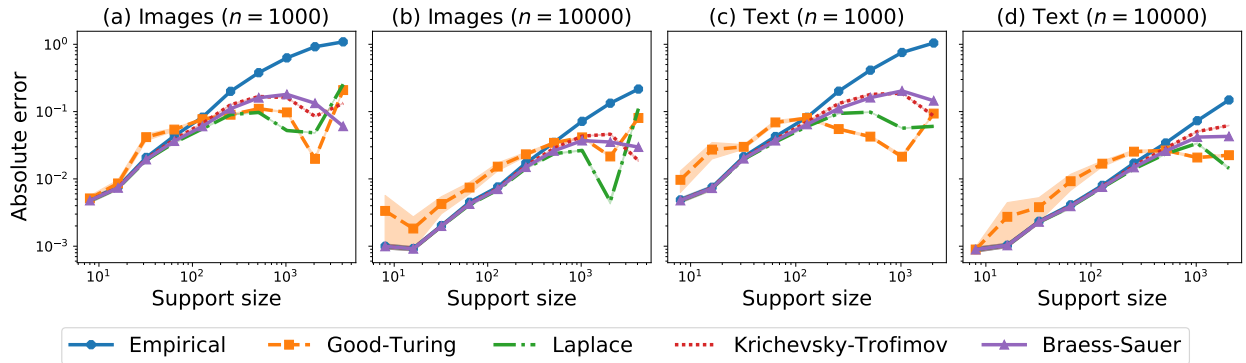


Figure 18: Absolute error versus support size  $k$  for different distribution estimators. **Left Two:** Image data (CIFAR-10) with sample sizes  $n = 1000$  and  $n = 10000$ . **Right Two:** Text data (WikiText-103) with sample sizes  $n = 1000$  and  $n = 10000$ .

**Setup** Let  $P, Q$  be two distributions on a finite alphabet  $\mathcal{X}$ . Recall that the divergence frontier is defined as the parametric curve  $\mathcal{F}(P, Q) := (x(\lambda), y(\lambda))$  for  $\lambda \in (0, 1)$  where

$$\begin{aligned} x(\lambda) &= \text{KL}_{1-\lambda}(Q\|P) = \sum_{a \in \mathcal{X}} Q(a) \log \frac{Q(a)}{\lambda P(a) + (1-\lambda)Q(a)} \\ y(\lambda) &= \text{KL}_\lambda(P\|Q) = \sum_{a \in \mathcal{X}} P(a) \log \frac{P(a)}{\lambda P(a) + (1-\lambda)Q(a)}. \end{aligned} \tag{24}$$

Recall that the Jeffery divergence between  $P$  and  $Q$  is defined as

$$\text{JD}(P, Q) = \text{KL}(P\|Q) + \text{KL}(Q\|P) = \sum_{a \in \mathcal{X}} (P(a) - Q(a)) (\log P(a) - \log Q(a)).$$

Note that  $\text{JD}(P, Q)$  is unbounded when there exists an atom such that  $P(a) = 0, Q(a) \neq 0$  or  $P(a) \neq 0, Q(a) = 0$ .

We show that the length of the divergence frontier between  $P, Q$  is lower bounded by the corresponding Jeffrey's divergence, which can be unbounded.

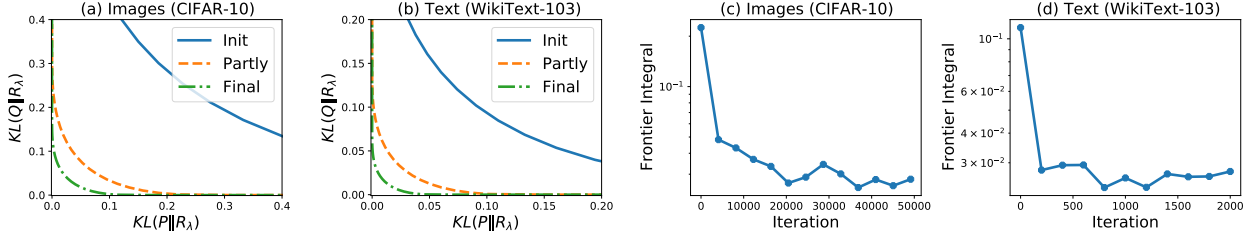


Figure 19: **Left Two:** The divergence frontier at different training checkpoints. **Right Two:** The frontier integral plotted at different training checkpoints.

**Proposition 28.** Consider two distributions  $P, Q$  on a finite alphabet  $\mathcal{X}$ . The length  $\text{length}(\mathcal{F}(P, Q))$  of the divergence frontier  $\mathcal{F}(P, Q)$  satisfies

$$\text{length}(\mathcal{F}(P, Q)) \geq \frac{1}{\sqrt{2}} \text{JD}(P, Q).$$

*Proof.* We assume without loss of generality that  $P(a) + Q(a) > 0$  for each  $a \in \mathcal{X}$ . Define shorthand  $R_\lambda = \lambda P + (1 - \lambda)Q$ . We bound the length of the divergence frontier  $\mathcal{F}(P, Q)$ , which is given by  $\int_0^1 L(\lambda) d\lambda$ , as

$$\begin{aligned} L(\lambda)^2 &= x'(\lambda)^2 + y'(\lambda)^2 \\ &= \left( \sum_{a \in \mathcal{X}} Q(a) \frac{Q(a) - P(a)}{R_\lambda(a)} \right)^2 + \left( \sum_{a \in \mathcal{X}} P(a) \frac{Q(a) - P(a)}{R_\lambda(a)} \right)^2 \\ &\geq \frac{1}{2} \left( \sum_{a \in \mathcal{X}} \frac{(P(a) - Q(a))^2}{R_\lambda(a)} \right)^2 =: \frac{1}{2} \tilde{L}(\lambda)^2, \end{aligned}$$

where we used the inequality  $(a - b)^2 \leq 2(a^2 + b^2)$  for  $a, b \in \mathbb{R}$ . We can now complete the proof by computing this integral as

$$\begin{aligned} \sqrt{2} \cdot \text{length}(\mathcal{F}(P, Q)) &\geq \int_0^1 \tilde{L}(\lambda) d\lambda \\ &= \int_0^1 \sum_{a \in \mathcal{X}} \frac{(P(a) - Q(a))^2}{R_\lambda(a)} d\lambda \\ &= \sum_{a \in \mathcal{X}} (P(a) - Q(a))^2 \int_0^1 \frac{1}{\lambda P(a) + (1 - \lambda)Q(a)} d\lambda \\ &= \sum_{a \in \mathcal{X}} (P(a) - Q(a))(\log P(a) - \log Q(a)) = \text{JD}(P, Q). \end{aligned}$$

□

## I Technical lemmas

We state here some technical results used in the paper.

**Theorem 29** (McDiarmid's Inequality). Let  $X_1, \dots, X_m$  be independent random variables such that  $X_i$  has range  $\mathcal{X}_i$ . Let  $\Phi : \mathcal{X}_1 \times \dots \times \mathcal{X}_m \rightarrow \mathbb{R}$  be any function which satisfies the bounded difference property. That

is, there exist constants  $B_1, \dots, B_n > 0$  such that for every  $i = 1, \dots, n$  and  $(x_1, \dots, x_n), (x'_1, \dots, x'_n) \in \mathcal{X}_1 \times \dots \times \mathcal{X}_n$  which differ only on the  $i^{\text{th}}$  coordinate (i.e.,  $x_j = x'_j$  for  $j \neq i$ ), we have,

$$|\Phi(x_1, \dots, x_n) - \Phi(x'_1, \dots, x'_n)| \leq B_i.$$

Then, for any  $t > 0$ , we have,

$$\mathbb{P}(|\Phi(X_1, \dots, X_n) - \mathbb{E}[\Phi(X_1, \dots, X_n)]| > t) \leq 2 \exp\left(-\frac{2t^2}{\sum_{i=1}^n B_i^2}\right).$$

**Property 30.** Suppose  $f : (0, \infty) \rightarrow [0, \infty)$  is convex and continuously differentiable with  $f(1) = 0 = f'(1)$ . Then,  $f'(x) \leq 0$  for all  $x \in (0, 1)$  and  $f'(x) \geq 0$  for all  $x \in (1, \infty)$ .

*Proof.* Monotonicity of  $f'$  means that we have for any  $x \in (0, 1)$  and  $y \in (1, \infty)$  that  $f'(x) \leq f'(1) = 0 \leq f'(y)$ .  $\square$

**Lemma 31.** For all  $x \in (0, 1)$  and  $n \geq 3$ , we have

$$0 \leq (1-x)^n x \log \frac{1}{x} \leq \frac{\log n}{n}.$$

*Proof.* Let  $h(x) = (1-x)^n x \log(1/x)$  be defined on  $(0, 1)$ . Since  $\lim_{x \rightarrow 0} h(x) = 0 < h(1/n)$ , the global supremum does not occur as  $x \rightarrow 0$ . We first argue that  $h$  obtains its global maximum in  $(0, 1/n]$ . We calculate

$$h'(x) = (1-x)^{n-1} \left( -nx \log \frac{1}{x} + (1-x) \left( \log \frac{1}{x} - 1 \right) \right) \leq (1-x)^{n-1} (1-nx) \log \frac{1}{x}.$$

Note that  $h'(x) < 0$  for  $x > 1/n$ , so  $h$  is strictly decreasing on  $(1/n, 1)$ . Therefore, it must obtain its global maximum on  $(0, 1/n]$ . On this interval, we have,

$$(1-x)^n x \log \frac{1}{x} \leq x \log \frac{1}{x} \leq \frac{\log n}{n},$$

since  $x \log(1/x)$  is increasing on  $(0, \exp(-1))$ .  $\square$

The next lemma comes from [2, Theorem 1].

**Lemma 32.** For all  $x \in (0, 1)$  and  $n \geq 1$ , we have

$$0 \leq (1-x)^n x \leq \exp(-1)/(n+1) < 1/n.$$